

Foraminiferal patterns in deglacial sediment in the western Ross Sea, Antarctica: life near grounding lines

Wojciech Majewski^{1*}, Lindsay O. Prothro^{2,3}, Lauren M. Simkins⁴, Ewa J. Demianiuk¹ and John B. Anderson²

¹ Institute of Paleobiology, Polish Academy of Sciences, Twarda 51/55, 00-818 Warszawa, Poland

² Department of Earth, Environmental and Planetary Science, Rice University, 6100 Main Street, Houston, TX 77005, USA

³ Department of Physical and Environmental Sciences, Texas A&M University - Corpus Christi, 6300 Ocean Drive, Corpus Christi, TX 78412

⁴ Department of Environmental Sciences, University of Virginia, 291 McCormick Drive, Charlottesville, VA, 22904, USA

Abstract

Improved multibeam swath bathymetry allows targeted coring of glacial landforms aiming at improving our understanding of sedimentary facies that developed in glacial settings during the post-Last Glacial Maximum (LGM) deglaciation. Coupled with radiocarbon dates, we explore foraminiferal records from eighteen sediment cores from the western Ross Sea largely from sites near paleo-grounding lines. We investigate post-LGM foraminiferal assemblages from glacial settings, including those proximal and more distal to paleo-grounding lines, including environments influenced by subglacial meltwater outflow and further removed from direct glacial influence and subject to different oceanographic conditions. Agglutinated benthic foraminiferal assemblages dominate open marine facies deposited under the presence of High Salinity Shelf Water and significant primary production, while calcareous foraminiferal assemblages characterize grounding line-proximal settings, some of which were potentially influenced by Modified Circumpolar Deep Water. Rapid deposition of meltwater plume deposits inhibited and, in some cases, significantly altered foraminifera abundance and diversity. Broadly in the Ross Sea, it appears that the high bathymetric gradient of grounding zone wedges is a key factor promoting rich benthic foraminiferal communities in habitats proximal to grounding lines. Therefore, we demonstrate that paleo-grounding line settings may archive high quality *in situ* foraminiferal data, which is imperative for paleoenvironmental and geochemical studies on glaciated continental margins worldwide.

1. Introduction

The Ross Sea is the largest drainage basin for the Antarctic Ice Sheet and has been the location of many marine geological studies. Despite the importance of the deglacial history of the Antarctic Ice Sheet in the Ross Sea and its contributions to sea level (e.g. DeConto & Pollard, 2016), the post-Last Glacial Maximum (LGM) history in this area is not adequately understood. Previous work suggests

that deglaciation in the Ross Sea could have started before the LGM (Mosola & Anderson, 2009; Bart & Cone, 2012), while a more recent review on the topic led to the interpretation that significant acceleration of the post-LGM deglaciation took place around 10,000 years ago (Anderson et al., 2014). More recent investigations have revealed a complex retreat scenario with individual ice streams showing different retreat patterns, timing, and sensitivity to different forcings (Greenwood et al., 2012, 2018; Jones et al., 2015; Halberstadt et al., 2016; Lee et al., 2017; Spector et al., 2017; Simkins et al., 2018; Prothro et al., 2020). The post-LGM glacial retreat in Pennell and JOIDES troughs, which are in the scope of this study, was also diachronous beginning at 15.1 and 13 calendar thousand years before present (cal ka BP), respectively (Prothro et al., 2020).

Complicating issues with such reconstructions stem from difficulties in obtaining precise age control due to poor understanding of sedimentary facies as they relate to specific glacial settings during ice sheet retreat, widespread reworking of sediments either during older glaciations or iceberg scouring of the seafloor (e.g., Andrews et al., 1999; Licht & Andrews, 2002; Mosola & Anderson, 2009), and limited preservation of carbonate (Kennett, 1968). Recent studies have focused on enhancing our understanding of sedimentary facies using improved multibeam swath bathymetry and targeted coring of glacial landforms that have not been scoured by icebergs and yield important information about the glacial setting during retreat (McGlannan et al., 2017; Prothro et al., 2018). Along with improvements to sediment facies distinctions, we must also understand foraminiferal assemblages and their habitats, as well as be able to distinguish *in situ* versus reworked specimens.

Previous studies have yielded considerable knowledge of modern foraminiferal assemblages from the Ross Sea (McKnight Jr., 1962; Pflum, 1966; Kennett, 1968; Osterman & Kellogg, 1979; Ward et al., 1987; Bernhard, 1987; Gooday et al., 1996; Violanti, 1996). Foraminiferal data, however, have been rarely employed in post-LGM paleoenvironmental reconstructions due to a poor understanding of species' ecology in near paleo-grounding line and sub-ice shelf settings (Brambati et al., 1999; Salvi et al., 2006; Melis & Salvi, 2009). Although studies of contemporary foraminifera from sub-ice shelf setting have taken place (e.g. Lipps et al., 1979; Pawlowski et al., 2005), they did not focus on understanding different assemblages. To fill this gap, studies relating foraminiferal assemblages to glacial landforms and sedimentary facies, that provide context for the glacial setting (e.g., Bart & Cone et al., 2012; Prothro et al., 2018), have successfully been used. A study conducted in the Whales Deep Basin in eastern Ross Sea (McGlannan et al., 2017) provided a robust paleoenvironmental framework for relating foraminiferal assemblages to near grounding-line and sub-ice-shelf settings. Majewski et al. (2018, 2019) found distinct agglutinated and calcareous assemblages in clearly different paleoenvironments and two rarely encountered morphotypes of pustulose *Globocassidulina bitor* and spinose *Trifarina earlandi* benthic foraminifera were found in abundance. These rare morphotypes appear to be restricted to extreme Antarctic environments with limited food resources, and hence are important potential paleoenvironmental indicators (Majewski et al., 2019). The major aim of this paper is to expand on the assessment of foraminiferal assemblages within the context of

paleo-grounding lines and deglacial sediments in the western Ross Sea. This work allows for the identification of environments where high-quality foraminiferal data can be obtained for paleoenvironmental reconstructions and radiocarbon dating, providing a better basis for site selection in future studies and constraints on glacial and marine processes active during ice sheet retreat.

1.1. Study area

Approximately a quarter of the Antarctic Ice Sheet drains into the Ross Sea from both the West Antarctic Ice Sheet (WAIS) and East Antarctic Ice Sheet (EAIS) (Figure 1A). Repeatedly throughout the late Cenozoic, paleo-ice streams from both ice sheets carved large bathymetric troughs within rift basins filled by thick sedimentary strata (Cooper et al., 1991; Anderson et al., 2019). During the LGM, large ice streams flowing through these troughs formed glacial lineations that record paleodrainage of the expanded ice sheet (e.g., Bart & Cone, 2012; Halberstadt et al., 2016). As the ice sheet retreated across the continental shelf, it left a geomorphic record of complex grounding line retreat patterns (Shipp et al., 1999; Greenwood et al., 2012, 2018; Halberstadt et al., 2016; Lee et al., 2017; Simkins et al., 2018) and a sedimentary succession composed of till overlain by glacial marine facies that document a temporal shift from ice-contact to ice-proximal to open-marine conditions (e.g., Domack et al., 1999). With the use of high-resolution multibeam bathymetry surveys, targeted sediment coring has shed light on distinct depositional changes with increasing distance from paleo-grounding lines and major refinements to sedimentary facies models (McGlannan et al., 2017; Prothro et al., 2018).

In addition to glacially influenced sedimentation on the Ross Sea continental shelf, oceanographic processes (e.g., Dunbar et al., 1985) play an increasingly important role in sedimentary processes as the ice sheet retreats landward. Relatively warm Modified Circumpolar Deep Water (MCDW) impinges onto the continental shelf at relatively high velocities compared to generally weak thermohaline currents on the inner shelf (Jacobs et al., 1974; Picco et al., 1999). The MCDW associated currents are strongest on the outer shelf and along the eastern sides of troughs, while denser and sluggish shelf water is directed northwards along the western sides of troughs (Orsi & Wiederwohl, 2009). The vigorous MCDW winnows fine terrigenous and biogenic sediment from the tops of the banks and outer shelf and deposits it on the inner shelf (Prothro et al., 2018). Another significant water mass is High Salinity Shelf Water (HSSW), the densest water mass in the Southern Ocean characterized by low temperatures around $-1.9\text{ }^{\circ}\text{C}$ and high salinities > 34.7 parts per thousand (Jacobs et al., 1985). Its production takes place during sea ice formation in polynyas and its presence effects the relatively shallow position of calcite compensation depth (CCD) in the western Ross Sea (Kennett, 1966). In the JOIDES and Pennell troughs (Figure 1A), Antarctic Surface Water increases in thickness from couple of tens of meters to up to ~ 100 m northwards as it flows above MCDW of similar thickness that flows onto the continental shelf at intermediate water depths. Most of the water column is occupied by HSSW, which ranges in thickness from 300 to 400 meters on the outer shelf to nearly 1000 m in southern Drygalski and JOIDES troughs (Orsi & Wiederwohl, 2009).

1.2. Ice sheet reconstruction and sedimentological framework

This study targeted coring sites across paleo-grounding lines, here recorded by grounding zone wedges (GZWs). The topsets of the GZWs record paleo-subglacial conditions, the foreset slopes of these landforms record ice-proximal conditions just seaward of the grounding line, such as sediment melt out from the base of the ice sheet and ice shelf as well as debris flows, and the toe or bottom set beds record glacial marine sedimentation at increasing distance from the grounding line (Figure 1C; Simkins et al., 2018). The maximum height of GZWs varies from less than 10 m to several tens of meters, which grow over periods of decades to a few thousand years (Bart et al., 2017; Simkins et al., 2017, 2018). Additional cores were collected from areas where mega-scale glacial lineations (MSGL) record subglacial conditions (Halberstadt et al., 2016).

We rely on the sedimentary facies model of Prothro et al. (2018), which is summarized in Figure 1C and distinguishes five different facies, as the paleoenvironmental framework for the foraminiferal record. Facies 1 is composed of massive diamicton acquired in cores taken from GZW topsets and from MSGL and is interpreted as till. Facies 2 was sampled in GZW foresets and is composed of diamicton with variable sorting and interpreted as debris flows initiated from GZW crests. Facies 3 is composed of diamicton with abundant granule- to pebble-sized soft sediment clasts, interpreted as an ice-proximal facies formed by basal melt out of debris-laden ice. Facies 4 is composed of relatively well-sorted silt with little or no ice-rafted debris, interpreted as meltwater plume deposits. Facies 5 is the most widespread facies, occupying the uppermost section of all cores, and is composed of olive-grey diatomaceous sandy silt; this facies records deposition in an open marine setting, similar to present-day conditions on the continental shelf seaward of the modern Ross Ice Shelf.

Initial foraminiferal data presented in (Prothro et al., 2018) show that some foraminiferal specimens were, in general, present in all five facies, with open marine diatomaceous sediments typically dominated by agglutinated foraminifera and all underlying facies (1 through 4) containing mostly calcareous foraminifera (Prothro et al., 2018). The largest proportion of clearly reworked specimens is found in facies 1 (till) and an elevated proportion of well-preserved specimens is seen in facies 2 (debris flow) and 3 (basal melt-out). The meltwater facies (facies 4) is often barren of foraminifera, most likely due to rapid deposition, but rarely contains an assemblage composed of minute benthic foraminifera. Here we expand on the work of Prothro et al. (2018) to provide more intra- and inter-regional variability in the eighteen core records that have been analyzed in the present study.

2. Materials and methods

2.1. Site selection and coring

Detailed micropaleontological analysis stems from eighteen kasten cores (KCs) recovered during the NBP1502a cruise onboard *Nathaniel B. Palmer RVIB* (Figure 1; Table 1). GZWs were the priority

sites of interest in the present study for coring; however, the slopes of banks and MSGL were also sampled to document a wide range of micropaleontological associations (Figure 2). At least three sediment cores were studied from four geographic areas in western Ross Sea: (a) southern Drygalski and JOIDES troughs, (b) just seaward of the LGM GZW in the north-central JOIDES Trough, (c) mid-Pennell Trough, and (d) seaward and landward of the LGM GZW in Pennell Trough (Figure 1A).

2.2. Sample processing

Sediment was taken every 10 cm from all cores and dried at room temperature, weighed, and washed through a 63 μm sieve. The dry-sieved $>125 \mu\text{m}$ fraction was routinely analyzed for foraminifera. In richer samples, dry residue was divided using a dry microsampler. The foraminiferal counts from the $>125 \mu\text{m}$ fraction were used for general overview of foraminiferal distribution patterns, using diversities (number of species per sample) of agglutinated vs. calcareous benthic foraminifera as well as their abundances (number of specimens per gram of dry sediment), supplemented with abundances of planktonic forms and clearly reworked specimens. The latter were identified based on having damaged tests, different coloration, and/or sediment filling (Majewski & Anderson, 2009), as well as representing extinct species (Webb & Strong, 2006). Specimens with pristine/fresh looking tests of extant species presently found in surface sediments of the Ross Sea were regarded as potentially *in-situ*.

The samples with the greatest potential for yielding reliable radiocarbon dates, i.e. showing high foraminiferal abundances and diversities as well as low numbers of clearly reworked specimens, were identified from the $>125 \mu\text{m}$ fraction. If possible, monospecific samples of >100 specimens of pristine looking tests from the $>300 \mu\text{m}$ fraction were isolated for each measurement. In samples with less abundant foraminifera, mixed benthics and/or planktonic *Neogloboquadrina pachyderma* sinistral foraminiferal samples were prepared and sent to the Mass Spectrometry facility of the University of Tokyo (Yokoyama et al., 2010) for radiocarbon dating. Details of most of the radiocarbon results are published in Prothro et al. (2020). Calibration of the radiocarbon ages was performed with Calib 7.0 and the Marine13 calibration curve (Stuiver and Reimer, 1993; Reimer et al., 2013) using a reservoir age of 1300 ± 100 years (Berkman and Forman, 1996). Two additional samples from KC13 (40–42 cm below core top) and KC24 (200–202 cm below core top) were sent for measurements to Poznań Radiocarbon Laboratory, Poland (Table 2). These radiocarbon dates were used to further assess the potential that the analyzed, pristine-looking foraminifera were *in situ*.

In order to analyze total foraminiferal assemblages from ice-proximal facies, the 63–125 μm fraction was also examined, however only in cores where reasonably abundant (>5 specimens per gram of dry sediment) pristine-looking specimens constitute post-LGM assemblages, which occurred in just four cores (KC17, KC30, KC48, and KC49). After picking, foraminiferal specimens from the 63–125 μm and $>125 \mu\text{m}$ fractions were arranged by taxa on micropaleontological slides and counted. The taxonomic approach followed that used by Majewski et al. (2018). This foraminiferal collection is

housed at the Institute of Paleobiology of the Polish Academy of Sciences (Warszawa) under the catalog number ZPAL F.71. Sediment samples from the same four cores that were processed for minute, i.e. 63–125 μm , foraminifera were also analyzed for granulometry. Along with the weights of entire dry samples, weights of dry-sieved residue were measured for the 63–125, 125–500, and >500 μm grain-size fractions.

To improve our understanding of the benthic foraminiferal assemblages, the combined foraminiferal abundances from the 63–125 μm and >125 μm fractions from the four cores were statistically analyzed using orthogonal rotated (Varimax) Q-mode principal component (PC) analysis with significant PC loading threshold of 0.4, according to Malmgren & Haq (1982) and Mackensen et al. (1990) and using a commercially distributed statistics package (SYSTAT 12). Taxa that constitute at least 1% of the total assemblage in at least a single sample were included in the matrix as well as samples with a total of at least 20 foraminifera. This low criterion allowed us to include large proportion of the samples in the statistical analysis, but carried a possibility of misinterpretation of the poorest samples. To avoid this, results of the PCA were crosschecked with unprocessed census data and sediment facies interpretation. The analyzed dataset, which included 39 taxa in 113 samples, comprised data from all the four cores analyzed, as they were taken from similar settings and, at least potentially, should provide a record of analogous foraminiferal assemblages. The PC scores showed the contribution of the selected variables (foraminiferal species) for each PC. Taxa that favored similar environmental conditions could have high scores on one PC, indicating their presence in one assemblage.

3. Results

3.1. Foraminiferal distribution by geographic regions

Foraminiferal distribution patterns from the >125 μm sediment fraction are quite geographically variable. In southern Drygalski and JOIDES troughs, cores were taken from a MSGL field (KC03), topsets of large (KC04) and small (KC05) GZWs, and the foresets of an intermediate size GZW (KC38) and a small GZW (KC43) (Table 1, Figure 2a). Cores from southern Drygalski Trough (KC03 and KC43) were taken from water depths greater (838 and 766 mwd [m water-depth]) than those of KC38 (681 mwd) and two sites from southern JOIDES Trough (KC04 and KC05 from ~600 mwd). In all five cores, the top-most open marine sediment was dominated by agglutinated foraminifera that showed moderate diversities (up to 10 species per sample) and abundances up to 38 specimens per gram of dry sediment, with a tendency to decrease down-core (Figure 3). In all cores except KC38, ~20 cm thick silt units, interpreted as meltwater plume deposits, were present directly below the open marine unit (Prothro et al. 2018). Like the open marine facies, these meltwater deposits were dominated by agglutinated foraminifera, but showed markedly lower diversities and abundances or were completely barren of foraminifera (KC04). The meltwater plume deposits in these four cores were underlain by tills. These tills were dominated by calcareous foraminifera, including minor

planktonic and visibly reworked tests, but their overall abundances only occasionally exceeded five specimens per gram of dry sediment. Diversities in the tills were low to moderate with up to 15 species per sample. Notably, foraminifera found in tills reached higher abundances and diversities in cores recovered from southern JOIDES Trough (KC04 and KC05) than from southern Drygalski Trough (KC03 and KC43). In this area, the only core recovered from an ice-marginal landform was KC38, in which proximal glacimarine debris flow deposits were identified below open marine deposits (Figure 3; Prothro et al., 2018). Foraminifera found in these proximal glacimarine deposits included very few agglutinated tests, excluding *M. areanacea*, which was usually common in open marine sediment facies (Appendix 1).

Three cores (KC30, KC48, and KC49) were recovered just north of the LGM grounding-line position in JOIDES Trough (Figure 2b). These cores were collected in similar water depths between 536 and 541 mwd from the foreset and toe of the LGM GZW (Table 1). In all three cores, sedimentary successions were similar, differing only in thickness of particular units (Figure 4). The open marine facies was dominated by agglutinated foraminifera that show moderate diversities (up to 10 species per sample) and abundances not exceeding 30 specimens per gram in the richest top samples. The underlying proximal glacimarine facies deposited through basal melt and debris flows were dominated by associations of calcareous foraminifera with significant numbers of planktonic foraminifera and only a few clearly reworked tests (Figure 4). It was not uncommon to count >15 different species per sample, with abundances typically reaching 5–10 specimens per gram of dry sediment. In the association dominated by calcareous foraminifera, the highest abundances (up to 30 specimens per gram) and diversities (up to 23 species) were noted in KC48.

Five cores were taken in the south-central part of the Pennell Trough (Figure 2c). Core KC13 was taken from the erosional meander of a paleo-subglacial channel. Core KC25 was taken from the toe and core KC27 was taken from the topset of a GZW at the mouth of this channel. In addition, KC19 was taken from the topset of a small GZW, and KC24 from the eastern slope of the Pennell Bank. All cores were collected in water depths between 450 and 456 m, except core KC13 which was taken from 575 mwd (Table 1). Open marine sediments were found to be present in the upper parts of all cores and range in thickness between ~40 cm in KC25 to at least 75 cm in KC13 (Figure 5). In south-central Pennell Trough, this facies was not always dominated by agglutinated foraminifera. They constituted only one third of the assemblage in the top of KC19, and were absent throughout the open marine sediments in KC13, where a diverse (>15 species per sample) and abundant (up to >1000 specimens per gram) calcareous assemblage, including planktonic foraminifera and lacking apparently reworked specimens, was present. Tills (in KC19 and KC27) and proximal glacimarine sediments (in KC25) occurred below the open marine sediments. Foraminifera in these facies were of low diversity, slightly exceeding 5 species per sample, and were strongly dominated by clearly reworked specimens. Core KC24 was unique because below the open marine facies was an almost 1 m thick interval of sediment with varied features characteristic of both meltwater plume and proximal glacimarine sediments

(Prothro et al., 2018). This part of the core, i.e. between 55 and 155 cm, was either barren in its middle part or included foraminiferal associations similar to those found in over- and under-lying sediments, but showing reduced diversities and abundances (Figure 5). The lowermost unit, well over 1 m thick, was identified as proximal glacimarine, including possible debris flow deposits, and contained moderately diverse (~10 species per sample) and abundant (up to 15 specimens per gram of dry sediment) calcareous foraminifera including minor planktonic and clearly reworked specimens (Figure 5).

In the central Pennell Trough, cores were taken near and on the large LGM GZW (Figures 1A and 2d). Cores KC14, KC15, and KC16 were taken from the foreset and topset of a GZW that marks a pause in post-LGM retreat of the grounding line; these cores showed slightly different facies successions but similar foraminiferal records and differed mainly in increasing thickness of units with dominant agglutinated foraminifera (open marine underlain by meltwater sediment) from <50 cm in KC14 to >100 cm in KC16 (Figure 6). Below this unit, a barren or nearly barren interval was identified as proximal glacimarine or ice shelf break-up facies (Prothro et al., 2018). The ice shelf break-up facies is not included in the generalized Prothro et al. (2018) facies scheme because it is geographically unique to KC16. It is characterized by a >30 cm section of concentrated ice-rafted debris not seen in other cores. Due to the typically clean nature of the Ross Ice Shelf, ice-rafted debris in the western Ross Sea is interpreted to represent calving of ice near or at the grounding line (Prothro et al., 2018). Below the barren sediments were intervals of proximal glacimarine (dominated by basal melt and debris flows), meltwater plume deposits, and till with low abundance associations dominated by benthic calcareous foraminifera of limited to moderate diversity (5–15 species per sample). Reworked foraminifera were clearly present but were not as abundant as in the south-central part of the Pennell Trough.

Core KC17, taken from the toe of the LGM GZW, and KC18, taken from its topset (Figure 2d, Table 1), were very different from the other central Pennell Trough cores in terms of their sediment and faunal characteristics. In KC17, below the open marine unit dominated by agglutinated foraminifera, a thick meltwater plume deposit interval is mostly barren of foraminifera. It is underlain by sediments sharing some characteristics of meltwater and proximal glacimarine facies, including debris flows, with a moderately diverse (10–15 species per sample) and abundant (up to 17 specimens per gram) assemblage dominated by calcareous benthic foraminifera and containing no clearly reworked specimens. Below this unit (between 225 and 270 cm bsf; below seafloor), proximal glacimarine deposits, including debris flows, exhibited a slightly more diverse (up to 18 species per sample) but much more abundant (up to >200 specimens per gram) assemblage dominated by calcareous benthic foraminifera and lacking clearly reworked tests. The lower-most core interval in KC17 was interpreted as open marine. It contains only a few foraminifera, which included agglutinated *M. arenacea*, typical of open marine sediments in most of other cores (Appendix 1). In contrast, >2 m of till occurred below the thin open marine surface unit in core KC18. It was found to

be almost barren below the uppermost 30 cm, with the exception of rare (<5 specimens per gram) and clearly reworked calcareous specimens (Figure 6).

3.2. Radiocarbon dates

Detailed information on the twenty-two radiocarbon results shown in Table 2 are in large part published in Prothro et al. (2020). Measurements from two samples from KC13 and KC24 were conducted in this study for evaluation of ages of the best preserved foraminifera in sites from the south-central part of the Pennell Trough. All foraminiferal dates were conducted on pristine-looking specimens and were used to further evaluate if they were from the last deglaciation. Only three measurements were not performed on foraminifera (Table 2).

The radiocarbon results are plotted in Figures 3–6. Initial drawdown of terrestrial ice adjacent to the Ross Sea has been reported to have occurred at least as early as 18 cal ka BP (Hall and Denton, 2000; Hall et al., 2013) and the end of the global LGM is generally accepted as ~20,000 years BP (e.g., Hughes et al., 2013). Thus, we estimate that *in situ* foraminifera, if collected from ice-proximal settings, should yield post-LGM ages of <20 000 years BP. If dates exceed ~20,000 years BP, they represent pre-LGM fauna or a mix of reworked and post-LGM specimens. As indicated in Table 2 and on Figure 3–6, the post-LGM ages were encountered only in KC17, KC30, KC48, and KC49. Thus, most of the well-preserved foraminifera in these sections are regarded as being *in situ*, with a slim possibility of only very minor admixture of well-preserved pre-LGM specimens. Based on the radiocarbon dates from these four cores (Table 2; Figures 4 and 6), it was also possible to estimate the duration of deposition of the proximal glacial marine sediments on LGM GZWs for at least 10,000 years.

3.3. Foraminiferal assemblages and granulometry

The four cores that yield rich post-LGM foraminiferal assemblages were analyzed for total foraminiferal assemblages, which integrate counts from the 63–125 μm and the >125 μm size fractions (Figure 7, Appendix 2). Five PCs account for 94.5 % of the total variance of the dataset (Figure 7, Table 3, Appendix 2). They are defined each by a single taxon with the highest positive PC scores. In three cases, all representing calcareous assemblages, the taxa with high PC scores were accompanied by taxa with lower, but still significant, positive scores or strongly negative, exceeding the value of -1.0, and thus contributing to the definition of the particular assemblage. The calculated PCs are referred to as foraminiferal assemblages (FAs) using the name of the dominant taxon. The two main PCs are (1) *Miliammina arenacea* FA, explaining 44.45% of the total variance in the dataset, and (2) *Globocassidulina subglobosa* FA, explaining 39.32% of total variance and showing additionally high scores of *Epistominella* spp. and *Globocassidulina biora*. Three additional FAs are considerably less widespread, i.e., (3) *Cassidulina* cf. *C. neoteretis* FA (5.00%) with high positive *Epistominella* spp. and negative scores of *G. biora* and *Trifarina earlandi*, (4) *Portachammina* spp. FA (3.15%), and (5)

Epistominella spp. FA (2.63%) with high negative scores for *G. subglobosa* and *Cassidulina* cf. *C. neoteretis*.

The FAs show similar changes in the four cores analyzed. The upper parts of the sections, represented by open marine facies, are dominated by agglutinated FAs, mostly the *M. arenacea* FA that could be substituted by the second agglutinated assemblage, i.e., the *Portatrochammina* spp. FA. In lower parts of all cores, where proximal glacimarine facies occur, calcareous FAs are present. They are dominated by the *G. subglobosa* FA. In the transitions from the proximal glacimarine to the open marine facies, the most rarely occurring calcareous assemblage, i.e. the *Epistominella* spp. FA may be present, while in KC17 the *Cassidulina* cf. *C. neoteretis* FA appears throughout the proximal glacimarine/meltwater facies interval between 140 and 230 cm bsf (Figure 7).

In all samples, the clay-to-silt grain-size (<63 μm) fractions dominates, constituting well over half of the sediment. Clay and silt fractions comprise >95% of sediment in most of the upper parts of the cores, representing open marine facies. The only exceptions are the lowest parts of the open marine units in all the four cores analyzed for total foraminiferal assemblages and the uppermost part of KC17, where the clay and silt are slightly less dominant, i.e. ~90%. With the exception of KC17, in proximal glacimarine facies, the >63 μm fraction constitutes 20–30 % of the sediment. In KC17, the meltwater plume deposits and proximal glacimarine with meltwater plume deposits are practically devoid of the >63 μm grain-size fraction.

4. Discussion

4.1. Foraminiferal distributions in relation to depositional setting

In the **till** facies (facies 1), associated with GZW topsets and MSGL fields, foraminifera show very low- to-moderate abundances and similarly variable diversities (Figures 3, 5, and 6). These characteristics, however, show strong regional variability. Tills are almost barren or have very few, mostly reworked specimens in the southern Drygalski Basin but exhibit slightly higher numbers, much higher diversities, and overall fewer clearly reworked specimens in the southern JOIDES Basin (Figure 3) and central Pennell Trough (KC18 on Figure 6). The low foraminiferal abundances and diversities in southern Drygalski correspond to a deeper water setting as compared to other sites, which likely contributes to poor calcium carbonate preservation. Foraminiferal associations from tills in KC19 and KC27 (south-central Pennell Trough, Figure 2c) are strongly dominated by clearly reworked foraminifera, possibly due to these two sites being proximal to a paleo-sub-glacial channel that would have mobilized an increased amount of subglacially reworked material to near the grounding line (Figure 2c).

Proximal glacimarine facies (facies 2 and 3) occur where sedimentation is dominated by basal melt and debris flows emanating directly from the grounding line (Figure 1B), and particularly well represented in cores collected near the LGM GZWs in JOIDES and Pennell troughs (Figure 1A). The most abundant assemblages were found in the lower part of core KC17 from the north-central Pennell

Trough (Figure 6) and in cores KC30, KC48, and KC49 from north-central JOIDES Trough (Figures 2b and 4) where high abundances and diversities were observed. Similar rich foraminiferal assemblages were found in association with GZWs in the Whales Deep Basin in the eastern Ross Sea (Majewski et al. 2018). The abundance of foraminifera at these locations indicates that the GZW foreset was an environment suitable for foraminifera, although repeated mixing by debris flows is indicated by the presence of clearly reworked specimens and radiocarbon dates that are not in stratigraphic order in KC48 (Figure 4).

Radiocarbon dates obtained from KC14 and KC16 yielded pre-LGM ages (Table 2 and Figure 6), supporting a lack of significant foraminiferal production at these locations after the LGM. A striking contrast between rich post-LGM foraminiferal communities at KC17 and their virtual absence at core sites KC14 and KC15 (Figure 6) indicates that foraminifera flourished in grounding line proximal settings during LGM but not necessarily during early deglaciation. These results suggest that the critical factor could be open marine influence, facilitating nutrient advection. The larger LGM GZWs farther seaward on the continental shelf experienced stronger open marine influence over relatively longer periods of time, enabling the establishment of rich calcareous foraminiferal assemblages than did the smaller GZWs that record post-LGM retreat from the continental shelf marked by shorter phases of grounding line proximal conditions and more limited ocean influence. Still different foraminiferal presence in the proximal glacimarine facies was noted in south-central Pennell Trough (Figure 5), specifically at site KC25, which only sampled small numbers of pristine-looking tests and abundant clearly reworked specimens, probably resulting from weak open marine influence near the grounding line and subglacial erosion during the formation of the Pennell Channel (Figure 2c). Quite abundant pristine-looking foraminifera found in proximal glacimarine facies in KC24 yielded a pre-LGM radiocarbon age (Table 2 and Figure 5) and could have been transported downslope from Pennell Bank, where calcareous foraminifera are common in surface sediments (Osterman & Kellogg 1979).

The **meltwater plume deposit** facies (facies 4) is widespread within the southern basins (Figure 3) and north-central Pennell Trough (Figure 6). In the latter area, near the LGM grounding-line location, this facies shows highly variable thickness and differences in foraminiferal indices. It is dominated by abundant agglutinated species, typical for open marine facies (KC14 through KC16 on Figure 6), suggesting deposition of meltwater sediments in open marine conditions with no ice-shelf. In contrast, in KC17 the meltwater facies was dominated by agglutinated foraminifera only in the upper part. The barren section is indicative of rapid deposition and the section with calcareous foraminifera indicates deposition in less open water, possibly below ice-shelf or multi-year sea ice with conditions favorable for carbonate preservation. Thin intervals of meltwater facies in the southern Drygalski and JOIDES basins (Figure 3) contain foraminifera analogous to that from overlying open marine facies, but with strongly reduced abundances and diversities. It suggests dilution due to elevated sedimentation rates as well.

The **open marine** facies (facies 5) occurs in the upper parts of all cores. In the majority of cores, this facies is dominated by agglutinated foraminifera, indicating presence of cold and corrosive bottom water. Agglutinated foraminifera decrease in abundances and diversities downcore. This is due, at least in part, to their generally poor preservation potential. In the three cores from the north-central JOIDES Trough (Figure 2b), the open marine intervals are expanded, up to >200 cm in KC48 (Figure 4), reflecting longer duration of post-LGM open marine conditions on the outer continental shelf. This also suggests HSSW presence and increasing primary productivity westwards, a result of less sea-ice cover in the area during warmer months (Prothro et al., 2018). At these three sites, foraminiferal indices were quite stable throughout the open marine intervals. In the cores from two sites near the Pennell Channel (KC13 and KC19; Figure 2c), the open marine facies shows a considerable abundance of calcareous foraminifera (Figure 5). In KC13, recovered from a meander of the paleo-subglacial channel, they are especially abundant, numbering up to almost 1000 specimens per gram of dry sediment. Because these foraminifera provided >40 ka BP radiocarbon ages (Table 2), they are interpreted as pre-LGM.

4.2. Foraminiferal assemblages from near grounding-line environments

The total foraminiferal counts from the four cores showing post-LGM *in situ* or syndepositional foraminifera, reveals five distinct FAs (Table 3). This includes three FAs that are dominated by calcareous species as well as two FAs dominated by agglutinated foraminifera. Paleoenvironmental conditions during dominance of these FAs, which are discussed below, are schematically visualized on Figure 8.

4.2.1. Arenaceous FAs from open marine facies. In the upper parts of cores KC17, KC30, KC48, and KC49 characterized as open marine diatomaceous facies (facies 5), two agglutinated FAs are dominated by *Miliammina arenacea* and *Portatrochammina* spp. (Figure 7). These two species often co-occurred and were occasionally accompanied by significantly less abundant *Paratrochammina bartrami*, *Recurvoides controtus*, as well as *Labrospira wiesneri*, *Textularia antarctica*, *Reophax spiculifer*, *Spiroplectammina biformis*, and other agglutinated species (Appendixes 2 and 3). These two FAs are similar to agglutinated assemblages identified in the eastern Ross Sea by Majewski et al. (2018). The association of agglutinated assemblages with the open marine facies was observed also in the George V-Adelie continental margin (Milam & Anderson, 1981) and the eastern Antarctic Peninsula (Ishman & Szymcek, 2003).

The *Miliammina arenacea* FA dominates the open marine facies, which is composed of diatomaceous sediments deposited during times of significant primary production and likely presence of HSSW (Figure 8D). The second agglutinated assemblage, *Portatrochammina* spp. FAs also appears to dominate during open-water conditions with possibly more intense ocean circulation causing moderate winnowing of organic-rich fine-grained sediments. However, this FA was statistically

significant only in uppermost samples of KC30 and KC49, and could be an artifact from relative fragility of *Portatrochammina* tests and stronger presence of *M. arenacea* down core due to its higher preservation potential (Schmiedl et al., 1997; Majewski & Anderson, 2009; Melis & Salvi, 2009). Thus, our *Portatrochammina* spp. FA may have no environmental significance.

The open marine facies were deposited at sites from 838 to 450 mwd (Table 1 and Figures 3-6) in similar to modern conditions, thus the paucity of calcareous foraminifera agrees with CCD, estimated in the recent western Ross Sea at ~430 mwd, where it seems to be related to presence of HSSW (Kennett, 1968). A similar relationship was found in the Weddell Sea (Anderson, 1975). HSSW production is known to occur in polynyas, which are especially persistent in Terra Nova Bay in the western Ross Sea (Kurtz & Bromwich, 1985), and is associated with sinking of high salinity waters enriched in CO₂ that further enhances corrosion of carbonates (Rysgaard et al., 2011).

4.2.2. *Globocassidulina subglobosa* FA. The most widespread calcareous FA in the western Ross Sea is the *G. subglobosa* FA. Accessory taxa are primarily *Epistominella* spp., *Globocassidulina biora*, *Cibicides* spp., *Nonionella* spp., *T. earlandi* (see also Appendixes 2 and 3) and, in KC17, agglutinated *Textularia* sp., the same species as in figure 2r of Bart et al. (2016). This FA is mainly associated with proximal glacial marine deposits (Figure 7). It is less dominant in core KC17 from Pennell Trough, especially in intervals lacking a coarser (>63 µm) fraction (Figure 7). A similar assemblage dominated by *G. subglobosa* was described by Melsi & Salvi (2009) from proximal glacial marine sediments of the western Ross Sea and in Glomar Challenger Basin in the eastern Ross Sea (Bart et al., 2016).

Despite different nominative taxa, the *G. subglobosa* FA could be closely related to the *G. biora* assemblage from the Whales Deep Basin (Majewski et al., 2018). *Globocassidulina biora* does occur within the *G. subglobosa* FA from the western Ross Sea (Table 3). *Globocassidulina subglobosa* and *G. biora* are commonly recognized as distinct species (e.g., Osterman & Kellog, 1979; Ward et al., 1987; Ishman & Domack, 1994; Melis & Salvi, 2009; Rodrigues et al., 2010; Gooday et al., 2014), which is confirmed by recent molecular studies (unpublished results), but *G. subglobosa* can be easily mistaken with juvenile forms of *G. biora*, as the two show similar morphology (Majewski & Pawłowski, 2010). Consequently, if co-occurring, abundances of these two species of *Globocassidulina* are difficult to quantify.

Despite the complexity of the relationships between the two *Globocassidulina* species identified in the Ross Sea, the FA dominated by *Globocassidulina* may indicate strong glacial influence (Anderson, 1975; Majewski, 2005, 2010; Melsi & Salvi, 2009; Kilfeather et al., 2011), including cold water conditions and elevated or variable sedimentation rates. Yet, the dominance of minute, thin-walled specimens of this genus in the western Ross Sea is in contrast with the Whales Deep Basin, where larger specimens dominate (Majewski et al., 2018, 2019). While some researchers interpreted environmental stress as the reason of undersized foraminiferal fauna, others argued the opposite, that foraminifera tend to be smaller, but also more abundant, in optimal conditions as they easily reach

reproductive maturity (Boltovskoy & Wright, 1976). In our samples, *G. subglobosa* rarely reached >5 specimens per gram of dry sediment, indicating environmental conditions unsuitable for all species except for the opportunistic *G. subglobosa* FA. The thin-walled tests indicate episodic (Gooday, 1993) and limited (Corliss, 1979) food supply (Figure 8A).

4.2.3. *Epistominella* spp. FA. Another calcareous FA is dominated by *Epistominella* spp. and is characterized by under-representation of *G. subglobosa* and *Cassidulina* cf. *C. neoteretis*, showing negative PC scores in Table 3. Together with the nominative taxon, spinose morphotype of *T. earlandi* as well as *Astrononion echolsi*, *Stainforthia concava*, *Nonionella iridea*, *G. subglobosa* and other calcareous foraminifera may be present (Appendixes 2 and 3). This FA shows PC loadings greater than the statistically significant value of 0.4 (Malmgren & Haq, 1982) only in two narrow intervals at the transition between proximal glacial marine facies and open marine facies in KC30 and KC48 (Figure 7), suggesting that suitable habitats for the *Epistominella* spp. FA existed only during the early deglaciation.

Epistominella exigua, which is included in the *Epistominella* spp. FA, is known to be resistant to dissolution (Anderson, 1975; Ishman and Szymcek, 2003) and is considered a phytodetritus-exploiting taxon (Gooday, 1993), as supported by its presence in sediments from the continental slope of the western Ross Sea (Barbieri et al., 1999). The *Epistominella* spp. FA could correspond to the *Epistominella* spp. assemblage from the location of the collapsed Larsen-A Ice Shelf, where it was interpreted to be adapted to seasonal food input in a generally food-limited environment (Ishman & Szymcek, 2003). Thus, it seems that the *Epistominella* spp. FA from the north-central JOIDES Trough could be an opportunistic organism, taking advantage of reduced, probably discontinuous food delivery to the GZW foreset, possibly near the limits of open marine conditions (Figure 8B).

Quite intriguing is a possible link of this FA with the occasional presence of the CDW in north-central JOIDES Trough, which is suggested by the presence of a similar assemblage in central Pine Island Bay (Majewski et al., 2016), where CDW flows onto the inner shelf (e.g., Jacobs et al., 2011, 2012). If this link with CDW/MCDW is valid, it took place in direct association with the beginning of ice sheet retreat and could hint of a mechanism of glacial retreat in this area. In addition, the presence of spinose *T. earlandi*, limited only to the intervals where the *Epistominella* spp. FA dominated (Appendix 3), could point to similar processes like in the Whales Deep Basin, where the strong presence of *T. earlandi* seems to be tied with intense bottom currents prior to the ice-shelf break up (Majewski et al., 2018).

4.2.4. *Cassidulina* cf. *C. neoteretis* FA. One of the most intriguing observations from our study relates to the *Cassidulina* cf. *C. neoteretis* FA. The nominative species of this FA – strongly flattened, lenticular *Cassidulina* from Antarctica (Figure 9) – is given various names by different authors: *C. carinata* Silvestri by Mead (1985), *C. neocarinata* Thalman by Kennett (1968), *C. laevigata*

d'Orbigny by Melis & Salvi (2009), *C. laevigata/teretis* by Mackensen et al. (1993), *C. teretis* Tappan by Mackensen and Douglas (1989) and Mackensen et al. (1990) and *C. neoteretis* Seidenkrantz by Kilfeather et al. (2011), possibly also *Cassidulina* spp. by (Ishman & Szymcek (2003). According to Seidenkrantz (1995), who established the *C. neoteretis* species, it closely resembles *C. carinata* and *C. laevigata*, as well as *C. teretis*. We found distinction between differently named lenticular *Cassidulina* problematic, requiring molecular methods to resolve the species.

Tentatively, we assume that all the lenticular *Cassidulina* described from numerous locations around Antarctica indeed represent a single species. This assumption is based on the molecular population structures of other Antarctic foraminifera, showing single, widely distributed species (Majewski et al., 2015; Majda et al., 2018). Moreover, most genetically investigated Antarctic foraminifera from shallow-water settings exhibit genetic divergence between morphologically similar sister genotypes from the Antarctic continental shelf and from the northern hemisphere polar regions (Pawlowski et al., 2008) and/or just north of Drake Passage (Majda et al., 2018). Based on these factors, it is likely that neither of the species names previously used for lenticular Antarctic *Cassidulina*, which were originally established for northern hemisphere foraminifera, applies to the Antarctic species. With this in mind, we tentatively applied the species name used by Kilfeather et al. (2011), who reported a similar foraminiferal assemblage dominated by lenticular *Cassidulina* along with *G. bitor* from Marguerite Bay. The cf., meaning *conformis*, was added to give notice of the questions discussed above.

In the northern hemisphere, *Cassidulina neoteretis*, which is related but not necessarily identical with the southern hemisphere species discussed in this study, was found to be especially common during deglaciation (Mackensen & Hald, 1988; Jansen & Bjørklund, 1985), where it was regarded as an indicator of modified Atlantic Water, a relatively saline and warm bottom water mass on the shelf (e.g., Jennings & Helgadottir, 1994; Jennings et al., 2017). Later, in the Holocene, *Cassidulina neoteretis* was replaced by the infaunal *C. laevigata* (Murray, 1991), also regarded as associated with particular water masses (Seidenkrantz, 1995). In the Arctic, it is associated with fine-grained and organic rich terrigenous mud, cold temperatures ($\sim -1^{\circ}\text{C}$) and normal marine salinities of $\sim 35\%$ (Mackensen et al., 1985; Mackensen & Hald, 1988).

Similarly, in Antarctica, *Cassidulina* cf. *C. neoteretis* appears to be linked with relatively cold conditions. It was only occasionally or not at all reported from the South Shetlands and western coasts of the Antarctic Peninsula (Finger & Lipps, 1981; Ishman & Domack, 1994; Majewski, 2005, 2010; Majewski et al., 2016), but it was more frequently reported in cooler regions like in the Ross Sea (Kennett, 1968; Osterman & Kellogg, 1979; Melis & Salvi, 2009; Majewski et al., 2018), the Weddell Sea (Mackensen & Douglas, 1989; Mackensen et al., 1990; Murray & Pudsey, 2004), and on the East Antarctic shelf (Milam & Anderson, 1981; Igarashi et al., 2001). In the latter areas, cold and saline Antarctic Bottom Water is associated with agglutinated assemblages (e.g. Kennett, 1966; Anderson

1975), therefore the calcareous *Cassidulina* cf. *C. neoteretis* FA may be associated with not as cold (i.e., relatively moderate) bottom water.

In the Ross Sea, the *Cassidulina* cf. *C. neoteretis* FA shows high PC loadings only in the lower part of KC17 where it co-occurs with abundant *G. subglobosa* FA (Appendix 2). Although *Cassidulina* cf. *C. neoteretis* strongly dominates its FA, it co-occurs with minor *G. subglobosa*, *Epistominella* spp., as well as agglutinated *Textularia* sp. (Appendix 3) but it is characterized by strongly negative PC scores of *G. biora* and *T. earlandi*. This fauna is associated with fine silt that is interpreted as a meltwater plume facies deposited in an ice proximal setting (Figure 7). Kilfeather et al. (2011) noted a similar faunal and sediment facies association, but with both *G. biora* and *G. subglobosa*, in a single core GC002 from Marguerite Bay, which they interpreted as a meltwater-derived, sub-ice-shelf deposit, consistent with our observations.

Unfortunately, no direct ecological data are available for *Cassidulina* cf. *C. neoteretis* and, interestingly, except in Marguerite Bay (Kilfeather et al., 2011), this Antarctic species is nowhere reported as a dominant species. A question to be asked is what ecological conditions during meltwater deposition allows for the development of such a unique assemblage, dominated by otherwise accessory species? Hypothetically, this assemblage could be associated with variable salinities caused by intermittent outflow of meltwater. This might explain its occurrence in both the western Ross Sea and Marguerite Bay where meltwater deposits are prevalent. This species was also present in subfossil assemblages from Pine Island Bay (unpublished results) (Figure 9) where subglacial meltwater deposits dominate surface sediments on the inner shelf and within basins on the middle self (Witus et al., 2014). Clearly, this species is especially suited to cope with increased sedimentation of fine-grained deposits. The three regions where *Cassidulina* cf. *C. neoteretis* has been reported, however, are also known for recent and historical presence of CDW (Jacobs et al., 1974, 1985, 2011, 2012; Kilfeather et al., 2011). Because of the strong link of the northern hemisphere of *C. neoteretis* with modified Atlantic Water (Jennings & Helgadottir, 1994; Jennings et al., 2017), we hypothesize that in the western Ross Sea, *Cassidulina* cf. *C. neoteretis* could be also linked with the presence of relatively warm and saline MCDW (Figure 8 C).

4.3. Abundant *in-situ* foraminifera suitable for radiocarbon dating

Our results confirm that proximal glaci-marine facies have the potential to bear *in-situ* foraminifera when collected from foresets and toes of GZWs in the western Ross Sea, supporting previous studies in the eastern Ross Sea (Bart & Cone, 2012; Bart et al., 2016; Majewski et al., 2018; Bart et al., 2018). However, abundant, post-LGM foraminifera were encountered only in the four cores (KC17, KC30, KC48, and KC49; Table 2, Figure 7). They are easily distinguished using foraminiferal indices based on the census data from the >125 µm fraction (Figures 4 and 6). In all four cases, calcareous foraminifera from the proximal glaci-marine facies exhibited moderate diversities, typically exceeding

15 species per sample, substantial abundances (>5 specimens per gram of dry sediment), as well as negligible numbers of clearly reworked specimens.

Foraminiferal indices show analogous patterns in the proximal glacial marine facies only in two other cores; in KC24 (Figure 5) and in the lowest part of KC14 (Figure 6). Thus, these assemblages could be also considered *in situ*. However, the radiocarbon measurements conducted on foraminiferal samples from these two cores provided old ages >30 cal ka BP (Table 2), suggesting either pre-LGM or mixed pre- and post-LGM fauna. These two examples show that foraminiferal indices cannot be used alone for distinguishing *in situ* calcareous foraminiferal assemblages that developed during the last deglaciation. Clearly, radiocarbon dating is needed to confirm *in-situ* or syndepositional character of analyzed foraminifera. The locations of sites with abundant calcareous assemblages in relation to the present day CCD (Kennett, 1966) is of no relevance as the current CCD seems to be mainly affected by HSSW and there is no reason to infer similar to modern oceanographic conditions on the continental shelf during early phases of deglaciation.

The rich calcareous assemblages post-dating LGM were found only in the four cores located at large GZWs deposited during and after the LGM (Figures 4 and 5). Furthermore, cores with almost barren (KC15, KC16, KC25, and KC38) or abundant, seemingly *in situ*, but largely pre-LGM calcareous foraminifera (KC14 and KC24), came from GZWs that are of much smaller size, reflecting shorter grounding line occupation durations and located farther away from the continental shelf edge than the LGM GZWs. Proximity to the continental shelf edge seemed to promote presence of rich calcareous assemblages (Taviani et al., 1993; Hauck et al., 2012; Majewski et al., 2018). More importantly, the high geomorphological gradient of GZWs formed during the LGM enabled a relatively thick water column between the decoupled ice sheet and the sea floor and likely more intense advection of bottom currents delivering food. The importance of open marine influence in developing rich calcareous benthic assemblages was previously noted in the Whales Deep (Majewski et al., 2018). In that study, isolated abundant calcareous foraminiferal assemblages were found only underneath an ice shelf on the northern, seaward side of a large and long-lived composite GZW, where a thick water column was influenced by open marine currents (Bart et al., 2017). Large LGM GZWs in the western Ross Sea also formed over a considerable timespans of thousands of years (Figures 4 and 5), providing enough time for stable benthic colonization (e.g., Alve, 1999).

4.4. Variable ice sheet behavior in the Ross Sea affecting foraminiferal record

There are significant differences in physiography and deglaciation patterns between the western and the eastern Ross Sea (e.g., Halberstadt et al., 2016). The WAIS, formerly occupying the eastern Ross Sea, is considered to be more dynamic, reacting faster to environmental change than the EAIS. The WAIS retreat from the continental shelf was marked by large-scale (tens of kilometers) back-stepping of the grounding line, as recorded by large GZWs separated by large stretches of sea floor with pristine MSGSL within troughs (Bart et al., 2017; Halberstadt et al., 2016). On the other hand, the

LGM grounding line of the EAIS in the western Ross Sea was characterized by large embayments within troughs on the outer continental shelf and its retreat from the shelf was dominated by multiple events that are recorded by small GZWs and moraines separated by tens of meters to a few hundred meters (Simkins et al., 2018), marking a high-frequency of smaller retreat events than in the eastern Ross Sea. This retreat style was in part driven by the rugged bathymetry of the western Ross Sea, characterized by multiple troughs and banks that acted as pinning points to the retreating grounding line (e.g., Anderson et al., 2014; Halberstadt et al., 2016). Based on our observations, the retreat behavior of the EAIS provided different ice-proximal marine settings that could be potentially inhabited by calcareous foraminifera. However, because of the short duration of the pauses in overall retreat, low relief of many GZWs, possible high sedimentation rates, and weak influence of open marine conditions, these ice-proximal environments could have been in large part unsuitable for calcareous foraminifera.

The calcareous FAs of the western Ross Sea are dominated by minute taxa, i.e., *G. subglobosa*, *Cassidulina* cf. *C. neoteretis*, and *Epistominella* spp. (Table 3), while those from the Whales Deep Basin in the eastern Ross Sea (Majewski et al., 2018) are composed mainly of *G. biora* and *T. earlandi*, of which adult individuals are among the largest calcareous forms in the Ross Sea (Majewski et al., 2019). These larger specimens developed in response to relatively stable living conditions on the outer continental shelf of the Whales Deep Basin due to a relatively thick water column, good exposure to oceanic circulation, and limited accumulation of organic-rich biogenic sediments and HSSW production that inhibit carbonate preservation. In the western Ross Sea, the dominance of opportunistic benthic foraminifera characterized by minute test sizes likely reflect limited water column thickness and oceanic influence, along with shorter durations of ice-proximal conditions. However, the LGM GZWs that developed in the JOIDES and Pennell troughs of the western Ross Sea (Figures 1A, 2b and 2d) provided habitats favorable for rich benthic communities (Figures 4 and 6).

Another important difference between the eastern and western Ross Sea is the more widespread presence of reworked calcareous foraminifera in tills from the western Ross Sea compared to practically barren subglacial tills in the Whales Deep Basin. In the latter, sub-ice-shelf facies contain foraminifera-bearing intervals including exclusively *in-situ* fauna (Majewski et al., 2018), while in the western Ross Sea, reworked microfossils are repeatedly noted (e.g., Kellogg et al., 1979; Webb & Strong, 1998; Melis & Salvi, 2009) as confirmed by this study (Figures 3-6). Clearly, strong reworking of microfossils in the western Ross Sea was due to erosion of fossiliferous strata demonstrated, for example, by the erosional channel passing through the location of KC13 (Figure 2c) and lateral transport either from biogenic carbonates on the outer continental shelf or from banks (Taviani et al., 1993).

5. Conclusions

Two agglutinated FAs dominated by *Miliammina arenacea* or *Portatrochammina* spp., dominate open marine facies deposited under the presence of HSSW and significant primary production, while calcareous foraminiferal assemblages, in particular *Globocassidulina subglobosa* FA, characterize grounding line-proximal settings. The dominance of minute, thin-walled specimens appears to reflect limited and episodic food supply in these glacially-dominated environments, similar but not identical to assemblages found in the eastern Ross Sea. The least common *Epistominella* spp. FA was prominent only at the transition between the grounding-line proximal glacimarine facies and the open marine facies, potentially linked with MCDW at the start of the deglacial conditions at paleo-grounding lines. We find typically uncommon *Cassidulina* cf. *C. neoteretis* to dominate another FA, showing a strong association with fine silt that is interpreted as a meltwater deposit facies occurring in ice-proximal settings. Similar assemblages have to date been described only in Marguerite Bay from a similar meltwater-derived, sub-ice-shelf deposit; however, based on both Antarctic and north Atlantic studies, CDW/MCDW presence may be also responsible for the *Cassidulina* cf. *C. neoteretis* FA.

Furthermore, based on foraminiferal indices and radiocarbon dates, high quality *in situ* calcareous foraminiferal material can be obtained from GZW foresets and toes that can be utilized for paleoenvironmental reconstructions and radiocarbon dating. Because foraminifera inhabited environments proximal to grounding lines, these *in situ* assemblages are capable of providing closer-than-ever-possible ages of grounding line retreat, important constraints on glacial processes, such as subglacial meltwater outflow, and on ocean conditions, as well as insight into ecological suitability of grounding line environments for benthic organisms.

Differences in the post-LGM foraminiferal record between the western and eastern Ross Sea manifest as dominance of minute taxa and widespread presence of clearly reworked specimens in the western Ross Sea. In the western Ross Sea, the combined influence of low relief of short-lived GZWs and weak influence of open marine conditions seem to have limited the suitability for colonization. By comparing spatial differences in foraminifera in the western and eastern Ross Sea, this study demonstrates that ice sheet retreat behavior, grounding line sedimentation and landform growth, as well as open ocean influence are dominant environmental controls on foraminifera assemblages and morphologies.

Acknowledgements

Fieldwork for this study was funded by a National Science Foundation Office of Polar Programs grant ANT-1246353 to John B. Anderson. Micropaleontological investigations were supported by grant of the National Science Centre, Poland NCN-2015/17/B/ST10/03346 to Wojciech Majewski. We would like to thank Grażyna Matriba and Olga Sánchez Vargas for help in sample processing. We also thank Marit-Solveig Seidenkrantz and two anonymous reviewers for their helpful comments that helped to improve this manuscript. All foraminiferal census data discussed in this paper are provided in the

Supporting Information that accompany this publication. They are also available in digital format at www.pangaea.de. This is a RCOM publication Nr. 10.1594/PANGAEA.911878.

References

- Alve, E. (1999). Colonization of new habitats by benthic foraminifera: a review. *Earth-Science Reviews*, 46, 167–185.
- Anderson, J.B. (1975). Ecology and distribution of foraminifera in the Weddell Sea of Antarctica. *Micropaleontology*, 21, 69–96.
- Anderson J.B. Conway H., Bart P.J., Witus A.E., Greenwood S.L., McKay R.M., Hall B.L., Ackert R.P., Licht K., Jacobsson M., & Stone, J.O. (2014). Ross Sea paleo-ice sheet drainage and deglacial history during and since the LGM. *Quaternary Science Reviews*, 100, 31–54.
- Anderson, J.B., Simkins, L.M., Bart, P.J., De Santis, L., Halberstadt, R.W., Olivo, E., Greenwood, & S., (2019). Seismic and geomorphic records of Antarctic Ice Sheet evolution in the Ross Sea and controlling factors in its behavior, in Glaciated Margins. In: Le Heron, D, D.P. Hogan, K.A., Philips, E.R., Huuse, M., Busfield, M.E. and Graham, A.G.C. (eds) Glaciated Margins: The Sedimentary and Geophysical Archive. *Geological Society, London, Special Publications*, 475, <https://doi.org/10.1144/SP475>.
- Andrews, J.T., Domack, E.W., Cunningham, W.L., Leventer, A, Licht, K.J., Jull, A.J.T., DeMaster, D.J., & Jennings, A.E. (1999). Problems and possible solutions concerning radiocarbon dating of surface marine sediments, Ross Sea, Antarctica. *Quaternary Research*, 52, 206–216.
- Barbieri, R., D'Onofrio, S., Melis, R., & Westall, F., (1999) r-Selected benthic foraminifera with associated bacterial colonies in Upper Pleistocene sediments of the Ross Sea (Antarctica): implications for calcium carbonate preservation. *Palaeogeography, Palaeoclimatology, Palaeoecology*, 149, 41–57.
- Bart, P. J., & Cone, A. N. (2012). Early stall of West Antarctic Ice Sheet advance on the eastern Ross Sea middle shelf followed by retreat at 27,500 14C yr BP. *Palaeogeography, Palaeoclimatology, Palaeoecology*, 335, 52–60.
- Bart P.J., Coquereau L., Warny S., & Majewski W. (2016). In situ foraminifera in grounding zone diamict: a working hypothesis. *Antarctic Science*, 28, 313–321.
- Bart, P.J., Krogmeier B.J., Bart M.P., & Tulaczyk S. (2017). The paradox of a long grounding during West Antarctic Ice Sheet retreat in Ross Sea. *Scientific Reports*, 7, 1262.
- Bart P.J., DeCesare, M., Rosenheim, B.E., Majewski, W., & McGlannan, A. (2018). A centuries-long delay between a paleo-ice-shelf collapse and grounding-line retreat in the Whales Deep Basin, eastern Ross Sea, Antarctica. *Scientific Reports*, 78, 12392
- Berkman, P.A., & Forman, S.L. (1996). Pre- bomb radiocarbon and the reservoir correction for calcareous marine species in the Southern Ocean. *Geophysical Research Letters*, 23, 363–366.
- Bernhard, J.M. (1987). Foraminiferal biotopes in Explorers Cove, McMurdo Sound, Antarctica. *Journal of Foraminiferal Research*, 17, 286–297.
- Boltovskoy, E., & Wright, R. (1976). Recent Foraminifera. Junk, The Hague, 515 p.
- Brambati, A., Fanzutti, G.P., Finocchiaro, F., Melis, R., Pugliese, N., Salvi, G., & Faranda, C. (1999). Some paleoecological remarks on the Ross Sea Shelf, Antarctica. In: Faranda F., Guglielmo E., Ianora A. (Eds.) Ross Sea Ecology, Italian Antarctic Expeditions (1987). Springer-Verlag, Berlin, 51–61.
- Cooper, A.K., Davey, F.J., & Hinz, K. (1991). Crustal extension and origin of sedimentary basins beneath the Ross Sea and Ross Ice Shelf. In: M.R.A. Thomson, J.A. Came, J.W. Thomson, eds, Geological Evolution of Antarctica, Cambridge University Press, New York, 285–291.
- Corliss, B.H. (1979). Size variation in the deep sea benthonic foraminifer *Globocassidulina subglobosa* (Brady) in the southeast Indian Ocean. *Journal of Foraminiferal Research*, 9, 50–60.
- DeConto, R.M., & Pollard, D. (2016). Contribution of Antarctica to past and future sea-level rise. *Nature*, 531, 591–597

- Domack, E.W., Jacobson, E.A., Shipp, S.S., & Anderson J.B. (1999). Late Pleistocene/Holocene retreat of the West Antarctic Ice-Sheet system in the Ross Sea: Part 2-Sedimentological and stratigraphic signature. *Geological Society of America Bulletin*, *111*, 1517–1536.
- Dunbar, R.B., Anderson, J.B., Domack, E.W., & Jacobs, S.S. (1985). Oceanographic influences on sedimentation along the Antarctic continental shelf. In: Jacobs, S.S. (Ed.), *Oceanology of the Antarctic Continental Shelf*, 291–312.
- Farmer, G.L., Licht, K., Swope, R.J., & Andrews, J. (2006). Isotopic constraints on the provenance of fine-grained sediment in LGM tills from the Ross Embayment, Antarctica. *Earth and Planetary Science Letters*, *249*, 90–107.
- Finger, K.L., & Lipps, J.H. (1981). Foraminiferal decimation and repopulation in an active volcanic caldera, Deception Island, Antarctica. *Micropaleontology*, *27*, 11–139.
- Gooday, A.J. (1993). Deep-sea benthic foraminiferal species which exploit phytodetritus: characteristic features and controls on distribution. *Marine Micropaleontology*, *22*, 187–205.
- Gooday, A.J., Bowser, S.S., & Bernhard, J.M. (1996). Benthic foraminiferal assemblages in Explorers Cove, Antarctica: A shallow-water site with deep-sea characteristics. *Progress in Oceanography*, *37*, 117–166.
- Gooday, A.J., Rothe, N., Bowser, S.S., & Pawlowski, J. (2014). Benthic foraminifera. In: De Broyer, C., Koubbi, P., Griffiths, H.J., et al. (Eds.), *Biogeographic Atlas of the Southern Ocean*. Scientific Committee on Antarctic Research, Cambridge, 74–82.
- Greenwood, S. L., Gyllencreutz, R., Jakobsson, M., & Anderson, J. B. (2012). Ice-flow switching and East/West Antarctic Ice Sheet roles in glaciation of the western Ross Sea. *Geological Society of America Bulletin*, *124*, 1736–1749.
- Greenwood, S.L., Simkins, L.M., Halberstadt, A.R.W., Prothro, L.O., & Anderson J.B. (2018). Holocene reconfiguration and readvance of the East Antarctic Ice Sheet. *Nature Communications*, *9*, 3176.
- Halberstadt, A.R.W., Simkins, L.M., Greenwood, S.L., & Anderson, J.B. (2016). Past ice-sheet behaviour: retreat scenarios and changing controls in the Ross Sea, Antarctica. *Cryosphere*, *10*, 1003–1020.
- Hall, B.L., & Denton, G.H. (2000). Radiocarbon chronology of Ross Sea drift, eastern Taylor Valley, Antarctica: evidence for a grounded ice sheet in the Ross Sea at the last glacial maximum. *Geografiska Annaler*, *82A*, 305–336.
- Hall, B.L., Denton, G.H., Stone, J.O., & Conway, H. (2013). History of the grounded ice sheet in the Ross Sea sector of Antarctica during the Last Glacial Maximum and the Last Termination. *Geological Society of London, Special Publication*, *381*, 167–181.
- Hauck, J., Gerdes, D., Hillenbrand, C.D., Hoppema, M., Kuhn, G., Nehrke, G., Völker, Ch., & Wolf-Gladrow, D. (2012). Distribution and mineralogy of carbonate sediments on Antarctic shelves. *Journal of Marine Systems*, *90*, 77–87.
- Hughes, P.D., Gibbard, P.L., & Ehlers, J. (2013). Timing of glaciation during the last glacial cycle: evaluating the concept of a global ‘Last Glacial Maximum’ (LGM). *Earth-Science Reviews*, *125*, 171–198.
- Igarashi, A., Numanami, H., Tsuchiya, Y., & Fukuchi, M. (2001). Bathymetric distribution of fossil foraminifera within marine sediment cores from the eastern part of Lützow-Holm Bay, East Antarctica, and its paleoceanographic implications. *Marine Micropaleontology*, *42*, 125–162.
- Ishman, S.E., & Domack, E.W. (1994). Oceanographic controls on benthic foraminifera from the Bellingshausen margin of the Antarctic Peninsula. *Marine Micropaleontology*, *24*, 119–155.
- Ishman, S.E., & Szymcek, P. (2003). Foraminiferal distributions in the former Larsen-A Ice Shelf and Prince Gustav Channel region, eastern Antarctic Peninsula margin: a baseline for Holocene paleoenvironmental interpretation. *Antarctic Research Series*, *79*, 239–260.
- Jacobs, S.S., Bauer, E.B., Bruchhausen, P.M., Gordon, A.L., Root, T.F., & Rosselot, F.L. (1974). Eltanin Report. Cruises 47–50, 1971; 52–55, 1972. In: Lamont-Doherty Geological Observatory of Columbia University Technical Report CU-2-74.
- Jacobs, S.S., Fairbanks, R.G., & Horibe Y. (1985). Origin and evolution of water masses near the Antarctic continental margin: Evidence from $\text{H}_2^{18}\text{O}/\text{H}_2^{16}\text{O}$ ratios in seawater. *Antarctic Research Series*, *43*, 59–85.

- Jacobs, S.S., Jenkins, A., Giulivi, C.F., & Dutrieux, P. (2011). Stronger ocean circulation and increased melting under Pine Island Glacier ice shelf. *Nature Geoscience*, 4, 519–523.
- Jacobs, S., Jenkins, A., Hellmer, H., Giulivi, C., Nitsche, F., Huber, B., & Guerrero, R. (2012). The Amundsen Sea and the Antarctic Ice Sheet. *Oceanography*, 25, 154–163.
- Jansen, E., Bjørklund, K. R. (1985). Surface ocean circulation in the Norwegian Sea 15.000 B.P. to present. *Boreas*, 14, 243–257.
- Jennings, A.E., & Helgadottir, G. (1994). Foraminiferal assemblages from the fjords and shelf of eastern Greenland. *Journal of Foraminiferal Research*, 24, 123–144.
- Jennings, A.E., Andrews, J.T., Ó Cofaigh, C., St. Onge, G., Sheldon, C., Belt, S.T., Cabedo-Sanz, P., & Hillaire-Marcel, C., (2017). Ocean forcing of Ice Sheet retreat in central west Greenland from LGM to the early Holocene. 472.
- Jones, R.S., Mackintosh, A.N., Norton, K. P., Golledge, N.R., et al. (2015). Rapid Holocene thinning of an East Antarctic outlet glacier driven by marine ice sheet instability. *Nature Communications*, 6, 8910.
- Kellogg, T.B., Osterman, L.E., & Stuiver, M. (1979). Late Quaternary sedimentology and benthic foraminiferal paleoecology of the Ross Sea, Antarctica. *Journal of Foraminiferal Research*, 9, 322–335.
- Kennett, J.P. (1966). Foraminiferal evidence for a shallow calcium carbonate solution boundary, Ross Sea, Antarctica. *Science*, 153, 191–193.
- Kennett, J.P. (1968). The fauna of the Ross Sea. Pt. 6. Ecology and distribution of Foraminifera. *New Zealand Department of Scientific and Industrial Research Bulletin*, 186, 1–47.
- Kilfeather, A.A., Ó Cofaigh, C., Lloyd, J.M., Dowdeswell, J.A., Xu, S., & Moreton, S.G. (2011). Ice-stream retreat and ice-shelf history in Marguerite Trough, Antarctic Peninsula: sedimentological and foraminiferal signatures. *Geological Society of America Bulletin*, 123, 997–1015.
- Kurtz, D.D., & Bromwich, D.H. (1985). A recurring, atmospherically forced polynya in Terra Nova Bay. In: Jacobs, S.S. (Ed.), *Oceanology of the Antarctic Continental Shelf*, 177–201.
- Lee, J.I., McKay, R.M., Golledge, N.R., Yoon, H.I., Yoo, K.C., Kim, H.J., & Hong, J.K. (2017). Widespread persistence of expanded East Antarctic glaciers in the southwest Ross Sea during the last deglaciation. *Geology*, 45, 403–406.
- Licht, K.J., & Andrews, J.T. (2002). The ^{14}C record of Late Pleistocene ice advance and retreat in the central Ross Sea, Antarctica. *Arctic Antarctic and Alpine Research*, 34, 324–333.
- Licht, K.J., Lederer, J.R., & Swope, J. (2005). Provenance of LGM glacial till (sand fraction) across the Ross embayment, Antarctica. *Quaternary Science Reviews*, 2, 1499–1520.
- Lipps, J.H., Ronan, T.E., & Delaca, T.E. (1979). Life below the Ross Ice Shelf, Antarctica. *Science*, 203, 447–449.
- Lowe, A.L., & Anderson, J.B. (2003). Evidence for abundant subglacial meltwater beneath the paleo-ice sheet in Pine Island Bay, Antarctica. *Journal of Glaciology*, 49, 125–138.
- Mackensen, A., & Douglas, R. G. (1989). Down-core distribution of live and dead deep-water benthic Foraminifera in box cores from the Weddell Sea and the California continental borderland. *Deep-Sea Research*, 36, 879–900.
- Mackensen, A., & Hald, M. (1988). *Cassidulina teretis* Tappan and *C. laevigata* d'Orbigny: Their modern and late Quaternary distribution in Northern Seas. *Journal of Foraminiferal Research*, 18, 16–24.
- Mackensen, A., Sejrup, H.P., & Jansen, E. (1985). The distribution of living benthic Foraminifera on the continental slope and rise off Southwest Norway. *Marine Micropaleontology*, 9, 27–5306.
- Mackensen, A., Grobe, H., Kuhn, G., & Fütterer, D.K. (1990). Benthic foraminiferal assemblages from the eastern Weddell Sea between 68 and 73°S: distribution, ecology and fossilization potential. *Marine Micropaleontology*, 16, 241–283.
- Mackensen, A., Fütterer, D.K., Grobe, H., & Schmiedl, G. (1993). Benthic foraminiferal assemblages from the eastern South Atlantic Polar Front region between 35° and 57°S: distribution, ecology and fossilization potential. *Marine Micropaleontology*, 22, 33–69.
- Majda, A., Majewski, W., Mamos, T., Grabowski, M., Godo, M.A., & Pawlowski, J. (2018). Variable dispersal histories across the Drake Passage: The case of coastal benthic Foraminifera. *Marine Micropaleontology*, 140, 81–94.

- Majewski, W. (2005). Benthic foraminiferal communities: distribution and ecology in Admiralty Bay, King George Island, West Antarctica. *Polish Polar Research*, 26, 159–214.
- Majewski, W. (2010). Benthic foraminifera from West Antarctic fiord environments: An overview. *Polish Polar Research*, 31, 61–82.
- Majewski, W., & Anderson, J.B. (2009). Holocene foraminiferal assemblages from Firth of Tay, Antarctic Peninsula: Paleoclimate implications. *Marine Micropaleontology*, 73, 135–147.
- Majewski, W., & Pawlowski, J. (2010). Morphologic and molecular diversity of the foraminiferal genus *Globocassidulina* in Admiralty Bay, West Antarctica. *Antarctic Science*, 22, 271–281.
- Majewski, W., Bowser, S.S., & Pawlowski, J. (2015). Widespread intra-specific genetic homogeneity of coastal Antarctic benthic foraminifera. *Polar Biology*, 38, 2047–2058.
- Majewski, W., Wellner, J.S., & Anderson, J.B. (2016). Environmental connotations of benthic foraminiferal assemblages from coastal West Antarctica. *Marine Micropaleontology*, 124, 1–15.
- Majewski, W., Bart, P.J., & McGlannan, A.J. (2018). Foraminiferal assemblages from ice-proximal paleo-settings in the Whales Deep Basin, eastern Ross Sea, Antarctica. *Palaeogeography, Palaeoclimatology, Palaeoecology*, 493, 64–81.
- Majewski, W., Stolarski J., & Bart, P.J. (2019). Two rare pustulose/spinose morphotypes of benthic foraminifera from eastern Ross Sea, Antarctica. *Journal of Foraminiferal Research*, 49, 405–422.
- Malmgren, B.A., & Haq, B.U. (1982). Assessment of quantitative techniques in paleobiogeography. *Marine Micropaleontology*, 7, 213–236.
- McGlannan, A., Bart, P., Chow, J., & DeCesare, M. (2017). On the influence of post-LGM ice-shelf loss and grounding zone sedimentation on West Antarctic Ice Sheet stability. *Marine Geology*, 392, 151–169.
- McKnight, W.M. Jr. (1962). The distribution of foraminifera off parts of the Antarctic coast. *Bulletins of American Paleontology*, 44, 65–158.
- Mead, G.A. (1985). Recent benthic foraminifera in the Polar Front region of the southwest Atlantic. *Micropaleontology*, 31, 221–248.
- Melis, R., & Salvi, G. (2009). Late Quaternary foraminiferal assemblages from western Ross Sea (Antarctica) in relation to the main glacial and marine lithofacies. *Marine Micropaleontology*, 70, 39–53.
- Milam, R.W., & Anderson, J.B. (1981). Distribution and ecology of recent benthonic foraminifera of the Adelie–George V continental shelf and slope, Antarctica. *Marine Micropaleontology*, 6, 297–325.
- Mosola, A.B., & Anderson, J.B. (2006). Expansion and rapid retreat of the West Antarctic Ice Sheet in eastern Ross Sea: possible consequence of over-extended ice streams. *Quaternary Science Reviews*, 25, 2177–2196.
- Murray, J.W. (1991). Ecology and palaeoecology of benthic foraminifera. Longman Scientific and Technical, 397 pp.
- Murray, J.W., & Pudsey, C.J. (2004). Living (stained) and dead foraminifera from the newly ice-free Larsen Ice Shelf, Weddell Sea, Antarctica: ecology and taphonomy. *Marine Micropaleontology*, 53, 67–81.
- Orsi, A.H., & Wiederwohl, C.L. (2009). A recount of Ross Sea waters. *Deep-Sea Research Part II: Topical Studies in Oceanography*, 56, 778–795.
- Osterman, L.E., & Kellogg, T.B. (1979). Recent benthic foraminiferal distribution from the Ross Sea, Antarctica: relation to ecologic and oceanographic conditions. *Journal of Foraminiferal Research*, 9, 250–269.
- Pawlowski, J., Fahrni, J.F., Guiard, J., Conlan, K., Hardecker, J., Habura, A., & Bowser, S.S. (2005). Allogromiid foraminifera and gromiids from under the Ross Ice Shelf: morphological and molecular diversity. *Polar Biology*, 28, 514–522.
- Pflum, C.E. (1966). The distribution of the foraminifera of the eastern Ross Sea, Amundsen Sea and Bellingshausen Sea, Antarctica. *Bulletins of American Paleontology*, 50, 151–209.
- Picco, P., Amici, L., Meloni, R., Langone, L., & Ravaioli M. (1999). Temporal variability of currents in the Ross Sea (Antarctica). In: G. Spezie, and G.M.R. Manzella (eds) *Oceanography of the Ross Sea, Antarctica*. Springer, New York, 103–117.

- Prothro, L., Simkins, L., Majewski, W., & Anderson, J. (2018). Glacial retreat patterns and processes determined from integrated sedimentology and geomorphology records. *Marine Geology*, *395*, 104–119.
- Prothro, L., Majewski, W., Yokoyama, Y., Simkins, L., Anderson, J., Yamane, M., Miyairi, T., & Ohkouchi, O. (2020). Timing and pathways of East Antarctic Ice Sheet retreat. *Quaternary Science Reviews*, *230*, 106166.
- Reimer, P.J., Bard, E., Bayliss, A., Beck, J.W., Blackwell, P.G., Ramsey, C.B., Buck, C.E., Cheng, H., Edwards, R.L., Friedrich, M., & Grootes, P.M. (2013). IntCal13 and Marine13 radiocarbon age calibration curves 0–50,000 years cal BP. *Radiocarbon*, *55*, 1869–1887.
- Rodrigues, A.R., Maluf, J.C.C., De Santis Braga, E., & Eichler, B.B. (2010). Recent benthic foraminiferal distribution and related environmental factors in Ezcurra Inlet, King George Island, Antarctica. *Antarctic Science*, *22*, 343–360.
- Rysgaard S., Bendtsen J., Delille B., Dieckmann G.S., Glud R.N., et al. (2011). Sea ice contribution to the air–sea CO₂ exchange in the Arctic and Southern Oceans. *Tellus B*, *63*, 823–830.
- Salvi, C., Busetti, M., Mariononi, L., & Brambati, A. (2006). Late Quaternary glacial marine to marine sedimentation in the Pennell Trough (Ross Sea, Antarctica). *Palaeogeography, Palaeoclimatology, Palaeoecology*, *231*, 199–214.
- Schmiedl, G., Mackensen, A., & Müller, P.J. (1997). Recent benthic foraminifera from the eastern South Atlantic Ocean: dependence on food supply and water masses. *Marine Micropaleontology*, *32*, 249–287.
- Seidenkrantz, M.S. (1995). *Cassidulina teretis* Tappan and *Cassidulina neoteretis* new species (Foraminifera): stratigraphic markers for deep sea and outer shelf areas. *Journal of Micropalaeontology*, *14*, 145–157.
- Shipp, S., Anderson, J., & Domack, E. (1999). Late Pleistocene–Holocene retreat of the West Antarctic Ice-Sheet system in the Ross Sea: part 1—geophysical results. *Geological Society of America Bulletin*, *111*, 1486–1516.
- Simkins, L.M., Anderson, J.B., Greenwood, S.L., Gonnermann, H.M., Prothro, L.O., Halberstadt, A.R.W., Stearns, L.A., Pollard, D., & DeConto, R.M. (2017). Anatomy of a meltwater drainage system beneath the ancestral East Antarctic ice sheet. *Nature Geoscience*, *10*, 691–697.
- Simkins, L.M., Greenwood, S.L., & Anderson, J.B. (2018). Diagnosing ice sheet grounding line stability from landform morphology. *Cryosphere*, *12*, 2707–2726.
- Spector, P., Stone, J., Cowdery, S.G., Hall, B., Conway, H., & Bromley, G. (2017). Rapid early-Holocene deglaciation in the Ross Sea, Antarctica. *Geophysical Research Letters*, *44*, 7817–7825.
- Stuiver, M., & Reimer, P.J. (1993). Extended ¹⁴C data base and revised CALIB 3.0 ¹⁴C age calibration program. *Radiocarbon*, *35*, 215–230.
- Taviani, M., Reid, D.E., & Anderson, J.B. (1993). Skeletal and isotopic composition and paleoclimatic significance of late Pleistocene carbonates, Ross Sea, Antarctica. *Journal of Sedimentary Research*, *63*, 84–90.
- Violanti, D. (1996). Taxonomy and distribution of recent benthic foraminifera from Terra Nova Bay (Ross Sea, Antarctica), Oceanographic Campaign 1987/1988. *Palaeontographia Italiana*, *83*, 25–71.
- Ward, B.L., Barrett, P.J., & Vella P. (1987). Distribution and ecology of benthic foraminifera in McMurdo Sound, Antarctica. *Palaeogeography, Palaeoclimatology, Palaeoecology*, *58*, 139–153.
- Webb, P.-N., & Strong, C.P. (1998). Recycled Pliocene Foraminifera from the CRP-1 Quaternary Succession. *Terra Antarctica*, *5*, 473–478.
- Webb, P.-N., & Strong, C.P. (2006). Foraminiferal biostratigraphy and palaeoecology in Upper Oligocene–Lower Miocene glacial marine sequences 9, 10, and 11, CRP-2/2A drill hole, Victoria Land Basin, Antarctica. *Palaeogeography, Palaeoclimatology, Palaeoecology*, *231*, 71–100.
- Witus, A.E., Braneky, C.M., Anderson, J.B., Szczuciński, W., Schroeder, D.M., Blankenship, D.D., & Jakobsson, M. (2014). Meltwater Intensive Glacial Retreat in Polar Environments and

Investigation of Associated Sediments: Example from Pine Island Bay, West Antarctica. *Quaternary Science Reviews*, 85, 99–118.

Yokoyama, Y., Koizumi, M., Matsuzaki, H., Miyairi, Y., & Ohkouchi, N. (2010). Developing ultra-small-scale radiocarbon sample measurement at the University of Tokyo. *Radiocarbon*, 52, 310–318.

Figure 1. Map of the western Ross Sea (**A**), showing areas of study: (a) south Drygalski and JOIDES troughs, (b) just seaward of the LGM GZW in the north-central JOIDES Trough, (c) mid-Pennell Trough, and (d) seaward and landward of the LGM GZW in the Pennell Trough with locations of cores analyzed in this study and line of bathymetric profile (**D**) showing location of coring sites along the Pennell Trough axis. Note inset maps showing location of this study in Antarctica and the Ross Sea, flow marks of the East (EAIS) and the West Antarctic Ice Sheet (WAIS), and asterisk indicating the location of the Whales Deep Basin (Majewski et al., 2018). Typical facies successions in cores (**B**), and sedimentary facies model of Prothro et al. (2018), demonstrating relationship of the five distinct facies to paleoenvironments (**C**).

Figure 2. Detailed sea-floor topography around core sites from south Drygalski and JOIDES troughs (**a1-a3**), just seaward of the LGM GZW in the north-central JOIDES Trough (**b**), from mid-Pennell Trough (**c**) and seaward and landward of the LGM GZW in the Pennell Trough (**d**).

Figure 3. Foraminiferal indices (>125 μm fraction) from cores KC3, KC4, KC5, KC38, and KC43 from south Drygalski and JOIDES troughs. The same core depth scale for all sections except KC38. Radiocarbon dates after Prothro et al. (2020).

Figure 4. Foraminiferal indices (>125 μm fraction) from cores KC30, KC48, and KC49 located just seaward of the LGM GZW in the north-central JOIDES Trough. The same core depth scale for all sections. Radiocarbon dates after Prothro et al. (2020).

Figure 5. Foraminiferal indices (>125 μm fraction) from cores KC13, KC19, KC24, KC25, and KC27 from mid-Pennell Trough. The same core depth scale for all sections except KC27. Radiocarbon dates after Prothro et al. (2020).

Figure 6. Foraminiferal indices (>125 μm fraction) from cores KC14 through KC18 located seaward and landward of the LGM GZW in the Pennell Trough. The same core depth scale for all sections. Radiocarbon dates after Prothro et al. (2020).

Figure 7. Total foraminiferal indices (>63 μm fraction) from cores KC17, KC30, KC48, and KC49, taken seaward of the LGM GZW, along with PC and granulometry results. PS loadings showing > 0.4 values are plotted on a single diagram for all FAs. Radiocarbon dates after Prothro et al. (2020).

Figure 8. Environmental conditions during development of FAs discussed in this study: (**A**) proximal glacial marine environment of LGM GZW foresets (dark grey) impacted by ocean circulation, causing limited and episodic food delivery, as well as a possible presence of moderately corrosive deep water seemed to constitute favorable conditions for the *Globocassidulina*

subglobosa FA; **(B)** stronger marine circulation, possibly delivering MCDW, and proximity to open water conditions resulted in more abundant than in the previous but still discontinuous food delivery favoring *Epistominella* spp. FA; **(C)** *Cassidulina* cf. *C. neoteretis* FA was associated exclusively with fine-grain meltwater deposits (orange) but it could be also linked with salinity changes due to MCDW; **(D)** in open water conditions, resulting in significant primary production and presence of corrosive HSSW, diatomaceous sediment (yellow) was dominated by agglutinated *Miliammina arenacea* FA accompanied by much less widespread *Portatrochammina* spp. FA. Graphics are not in scale. Environmental context of cores shown at the top of the panels.

Figure 9. SEM images of *Cassidulina* cf. *C. neoteretis* from the western Ross Sea: **1-3**. NBP15-2A, KC17, 260-262 cm; **4**. NBP15-2A, KC30, 250-252 cm; **5**. NBP15-2A, KC49, 160-162 cm; **6**. NBP15-2A, KC49, 257-259 cm; and from Pine Island Bay: **7-8**. OSO 0910, KC 15, core catcher. All scale bars equal 100 μ m.

Appendix 1. Foraminiferal census data from the >125 μ m sediment fraction.

Appendix 2. Total foraminiferal census data from the >63 μ m sediment fraction from four cores showing post-LGM in situ or syndepositional foraminifera.

Appendix 3. Core logs, foraminiferal assemblages, and abundances of selected foraminiferal taxa for KC17, KC30, KC48, and KC49 sections.

Table 1. Core locations. * Re-occupied site NBP9501 KC39 of Domack et al. (1999).

Core ID	Water depth (mwd)	Latitude	Longitude	Core length (cm)	Geomorphological setting
KC03	838	-76° 12.973'	164° 53.170'	269	MSGL
KC04	597	-76° 4.688'	170° 20.056'	200	Topset of large GZW topset
KC05	600	-76° 3.453'	170° 23.381'	266	Topset of small GZW topset
KC13	575	-76° 10.302'	175° 46.658'	81	Meander of subglacial Pennell Channel
KC14	554	-75° 55.470'	179° 6.755'	204	Toe of steep post-LGM GZW
KC15	558	-75° 55.481'	179° 6.510'	243	Foreset of steep post-LGM GZW
KC16	541	-75° 55.484'	179° 6.343'	288	Topset of steep post-LGM GZW
KC17	549	-75° 52.420'	179° 39.976'	278	Toe of LGM GZW
KC18	481	-75° 52.955'	179° 32.783'	270	Topset of LGM GZW
KC19	455	-76° 1.815'	177° 12.618'	290	Topset of small GZW
KC24	450	-75° 40.281'	176° 26.789'	295	Slope of Pennell Bank
KC25	456	-76° 1.901'	176° 50.866'	256	Toe of GZW/fan at Pennell Channel termination
KC27	451	-76° 2.634'	176° 39.710'	114	Backside of GZW/fan at Pennell Channel termination
KC30	536	-74° 26.863'	173° 22.787'	303	Topset or foreset of LGM GZW
KC38	681	-76° 14.921'	167° 15.535'	71	Foreset of middle GZW
KC43	766	-76° 19.150'	165° 19.742'	153	Small scale GZWs
KC48*	539	-74° 28.376'	173° 30.652'	315	Foreset of LGM GZW
KC49	541	-74° 22.360'	173° 34.797'	258	Toe of LGM GZW

Table 2. Radiocarbon dates from NBP15-02a cores. Dates have been calibrated with Calib 7.0 and the Marine13 calibration curve (Stuiver and Reimer, 1993; Reimer et al., 2013), with a reservoir age of 1300 ± 100 yr (Berkman and Forman, 1996).

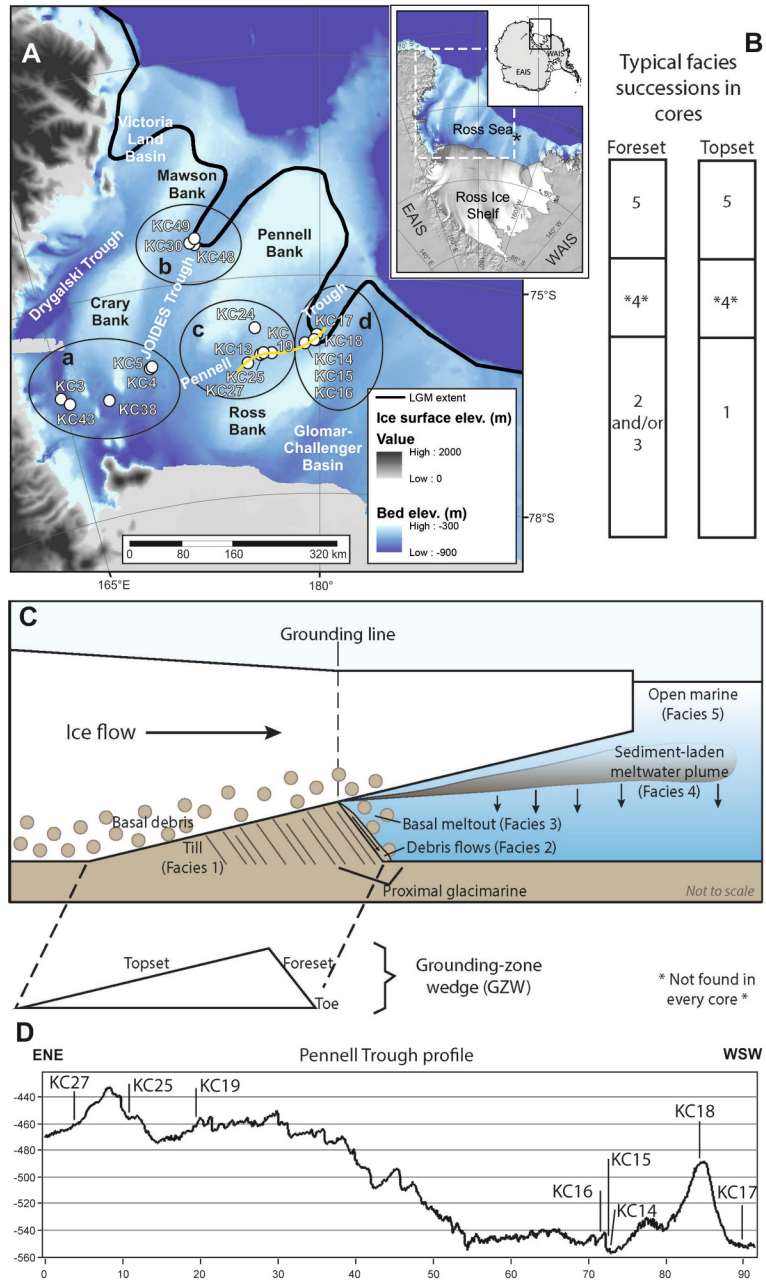
See separate file

Table 3. Foraminiferal PC scores. Taxa important for particular FAs are in bold.

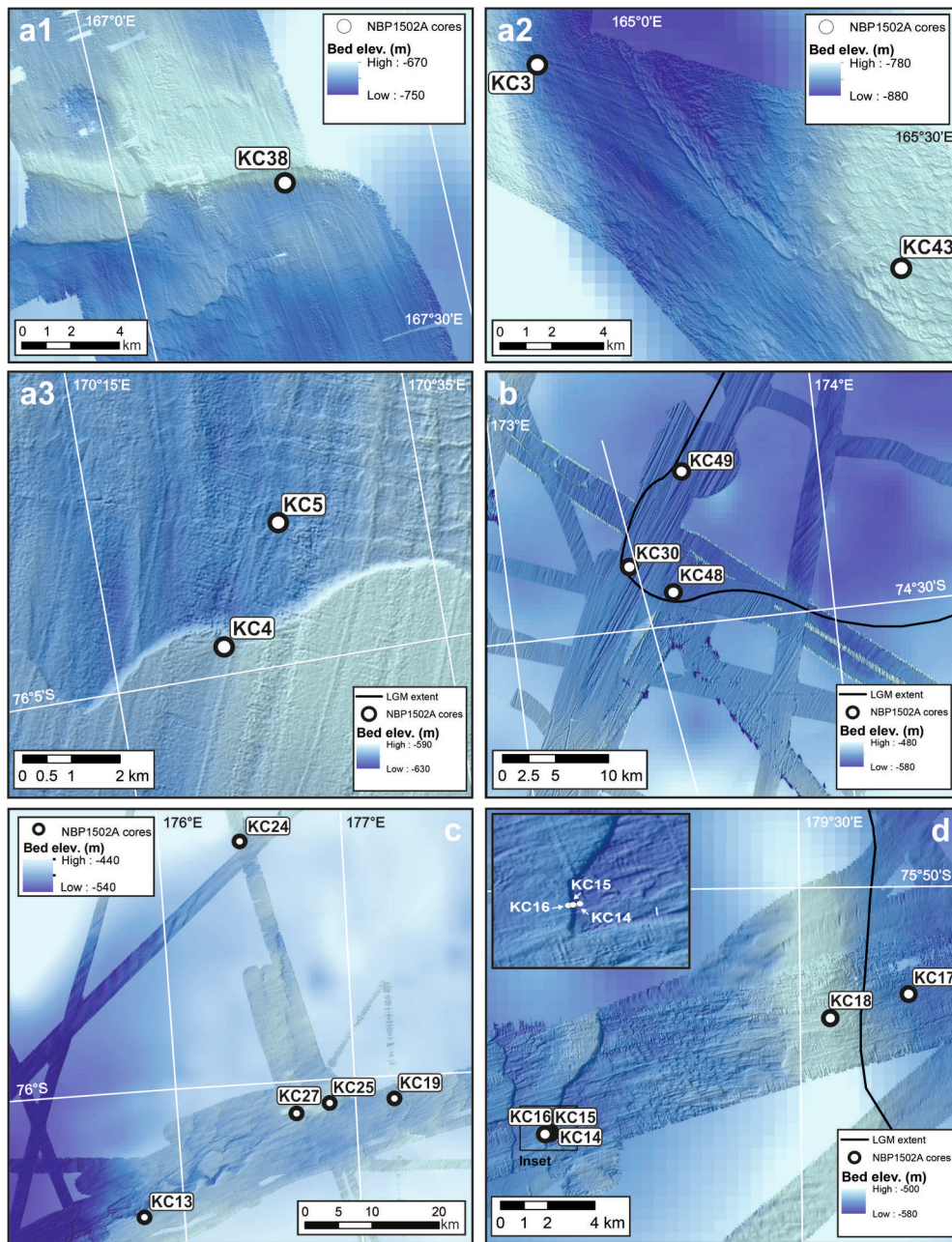
	<i>M. arenacea</i> FA	<i>G. subglobosa</i> FA	<i>Cassidulina</i> <i>cf. C. neoteretis</i> FA	<i>Portatrochammina</i> spp. FA	<i>Epistominella</i> spp. FA
Total variance explained (%)	44.45	39.32	5.00	3.15	2.63
<i>Miliammina arenacea</i>	6.05	-0.07	-0.04	-0.56	0.09
<i>Portatrochammina</i> spp.	0.41	-0.28	-0.16	5.73	-0.23
<i>Paratrochammina bartrami</i>	0.07	-0.34	-0.23	0.12	-0.39
<i>Spiroplectammina bififormis</i>	-0.19	-0.47	-0.15	-0.22	-0.20
<i>Labrospira wiesneri</i>	-0.21	-0.46	-0.16	0.23	-0.20
<i>Recurvoides contortus</i>	-0.14	-0.42	-0.00	0.58	-0.58
<i>Rhabdammina</i> spp.	-0.19	-0.46	-0.18	0.30	-0.28
<i>Hormosinella</i> spp.	-0.14	-0.46	-0.19	0.47	-0.33
<i>Reophax</i> spp.	-0.17	-0.46	-0.19	0.40	-0.32
<i>Reophax spiculifer</i>	-0.19	-0.46	-0.16	0.05	-0.22
<i>Textularia antarctica</i>	-0.19	-0.46	-0.16	0.02	-0.24
<i>Textularia</i> sp.	-0.19	-0.44	0.17	-0.37	-0.18
other agglutinated forams	-0.19	-0.46	-0.17	0.30	-0.24
<i>Cassidulinoides parkerianus</i>	-0.20	-0.34	-0.23	-0.34	-0.15
<i>Cassidulinoides</i> sp.	-0.20	-0.45	-0.14	-0.34	-0.16
<i>Cassidulina cf. C. neoteretis</i>	-0.11	-0.36	5.48	-0.41	-1.31
<i>Globocassidulina biora smooth</i>	-0.18	1.14	-1.19	-0.53	0.57
<i>G. biora pustulose</i>	-0.20	-0.45	-0.14	-0.35	-0.24
<i>Globocassidulina subglobosa</i>	-0.07	5.20	0.06	0.22	-2.65
<i>Ehrenbergina glabra</i>	-0.19	0.04	-0.47	-0.42	-0.15
<i>Trifarina earlandi costate</i>	-0.14	0.75	-1.09	-0.71	0.72
<i>T. earlandi spinose</i>	-0.18	-0.40	-0.10	-0.30	0.81
<i>Fursenkoina fusiformis</i>	-0.17	-0.22	-0.30	-0.36	-0.36
<i>Bolivinellina pseudopunctata</i>	-0.20	-0.45	-0.15	-0.33	-0.22
<i>Bolivinellina earlandi</i>	-0.20	-0.45	-0.16	-0.34	-0.24
<i>Stainforthia concava</i>	-0.20	-0.09	0.36	-0.13	0.33
<i>Astrononion echolsi</i>	-0.21	0.03	0.01	0.40	0.46
<i>Astrononion antarcticum</i>	-0.20	-0.33	-0.24	-0.39	-0.01
<i>Pullenia subcarinata</i>	-0.20	-0.39	-0.22	-0.39	-0.12
<i>Nonionella iridea</i>	-0.19	0.05	0.44	-0.29	-0.01
<i>Nonionella bradyi</i>	-0.16	0.57	-0.02	-0.45	0.48
<i>Nonionella</i> sp.	-0.20	-0.44	-0.16	-0.34	-0.19
<i>Epistominella</i> spp.	-0.17	1.84	1.74	0.55	5.00
<i>Ioanella tumidula</i>	-0.19	-0.42	-0.03	-0.36	-0.15
<i>Cibicides</i> spp.	-0.19	0.94	-0.85	-0.20	0.70
<i>Rosalina globularis</i>	-0.20	-0.19	-0.34	-0.34	0.06
lageninids	-0.20	0.25	-0.32	-0.21	0.39
miliolids	-0.20	-0.21	-0.31	-0.33	0.02
other calcareous forams	-0.20	-0.38	-0.02	-0.34	-0.26

core ID	interval (cm)	material	Lab_ID	Conventional ¹⁴ C age (yr BP)	SD (yr)	Calibrated age (cal yr BP)	SD (yr)
KC04	160-170	mix of ~400 different minute foraminifera	YAUT-037513	24762	172	27628	141
KC04	190-200	mix of ~400 different minute foraminifera	YAUT-037515	30180	307	33071	443
KC05	60-70	160 <i>G. biora</i> , 16 <i>C. cf. C. neoteretis</i> + 55 <i>N. pachyderma</i>	YAUT-037516	23848	175	26857	265
KC13	13.5-14.5	brachiopod	YAUT-015709	39997	159	42653	160
KC13	40-42	60 large <i>G. biora</i>	Poz-98390*	> 44 000	n/a		
KC14	200-202	12 <i>T. earlandi</i> + 4 <i>B. aculeata</i> + 40 <i>G. biora</i> + 10 <i>N. pachyderma</i>	YAUT-037518	30623	275	33520	302
KC16	170-180	45 benthics (mainly <i>G. biora</i>) + 20 <i>N. pachyderma</i>	YAUT-037517	22724	435	25671	460
KC17	130-140	10 other benthic+ 50 <i>G. biora</i> + 85 <i>N. pachyderma</i>	YAUT-037509	14162	81	15366	204
KC17	140-150	110 <i>G. biora</i> , 100 <i>C. cf. C. neoteretis</i> + 120 <i>N. pachyderma</i>	YAUT-037512	14035	100	15121	273
KC17	240-250	150 <i>G. biora</i> + 120 <i>N. pachyderma</i>	YAUT-031624	24613	87	27545	110
KC17	250-260	150 <i>G. biora</i> + 175 <i>N. pachyderma</i>	YAUT-032412	28854	95	31330	112
KC24	200-202	40 <i>N. pachyderma</i> + 80 <i>G. biora</i>	Poz-98389*	31500	500		
KC30	130-132	20 <i>T. earlandi</i> + 42 <i>N. pachyderma</i>	YAUT-038429	11882	102	12476	183
KC30	290-292	30 mixed benthic foraminifera	YAUT-038304	21457	115	24220	184
KC48	220-222	23 <i>G. biora</i> , 10 <i>F. fusiformis</i> + 18 <i>N. pachyderma</i>	YAUT-038436	14166	115	15378	239
KC48	220-230	54 <i>N. pachyderma</i> + 70 various benthics	YAUT-016821	17446	129	19453	220
KC48	250-260	170 <i>N. pachyderma</i>	YAUT-016823	14904	411	16431	613
KC48	250-260	180 <i>Globocassidulina</i>	YAUT-016822	19877	143	22447	199
KC48	310-315	brachiopod	YAUT-015713	16003	42	17876	143
KC48	317-319	150 <i>N. pachyderma</i>	YAUT-016824	12751	86	13315	125
KC49	150-152	fragmented brachiopod	YAUT-038232	11326	50	11532	221
KC49	220-222	36 mixed benthic foraminifera	YAUT-038303	22566	131	25610	172

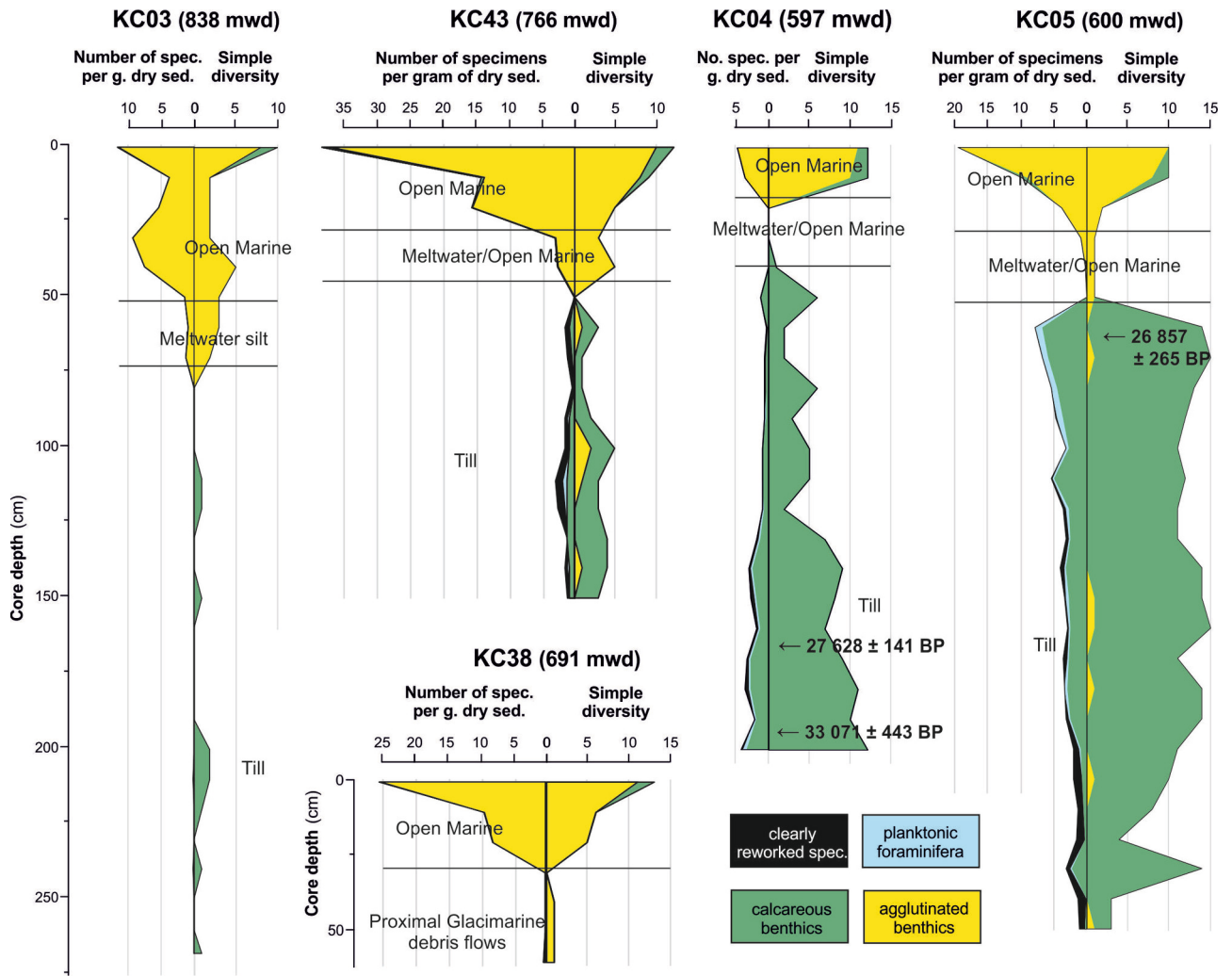
* performed in Poznań Radiocarbon Laboratory



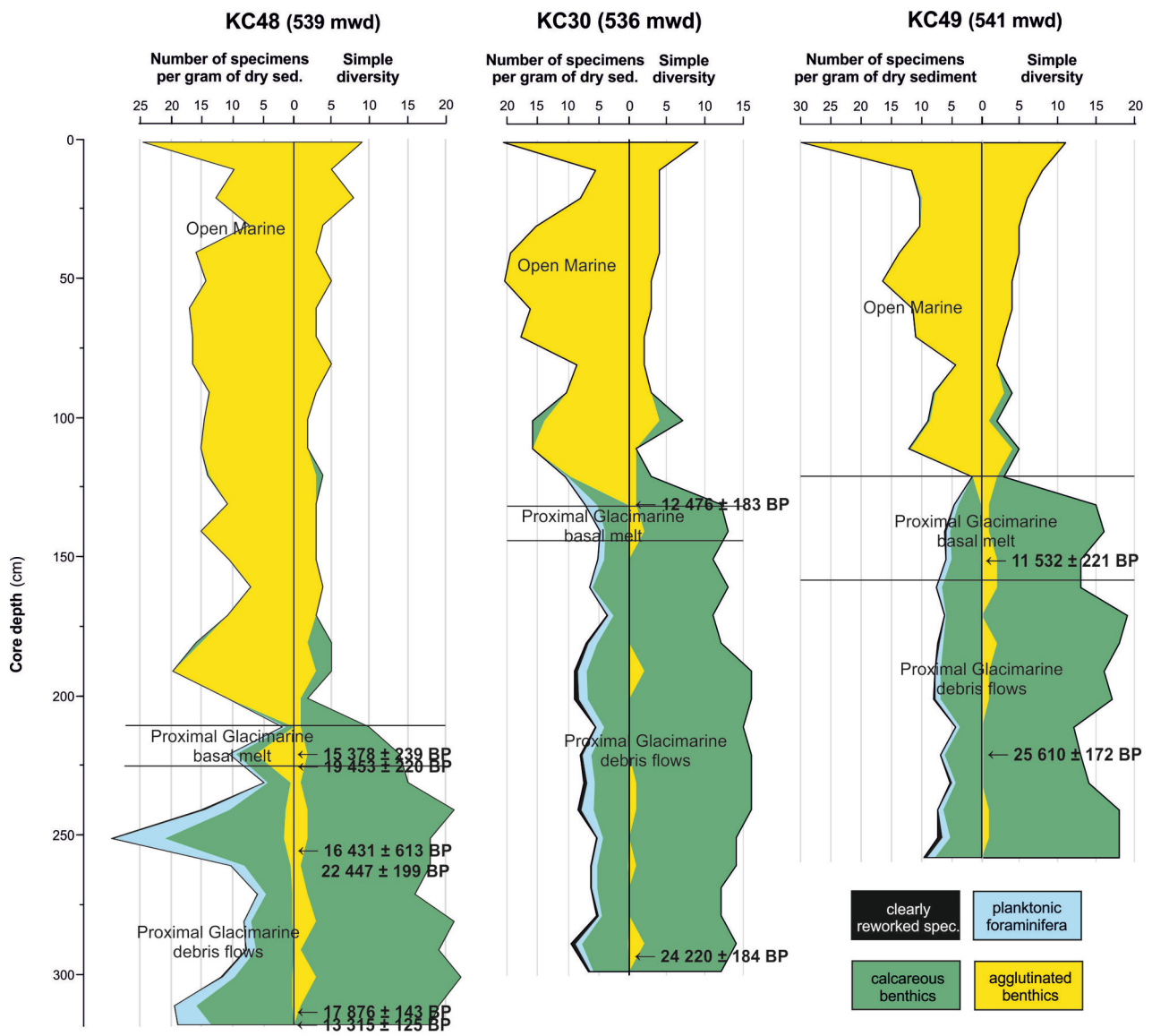
2019PA003716-f01-z-.jpg



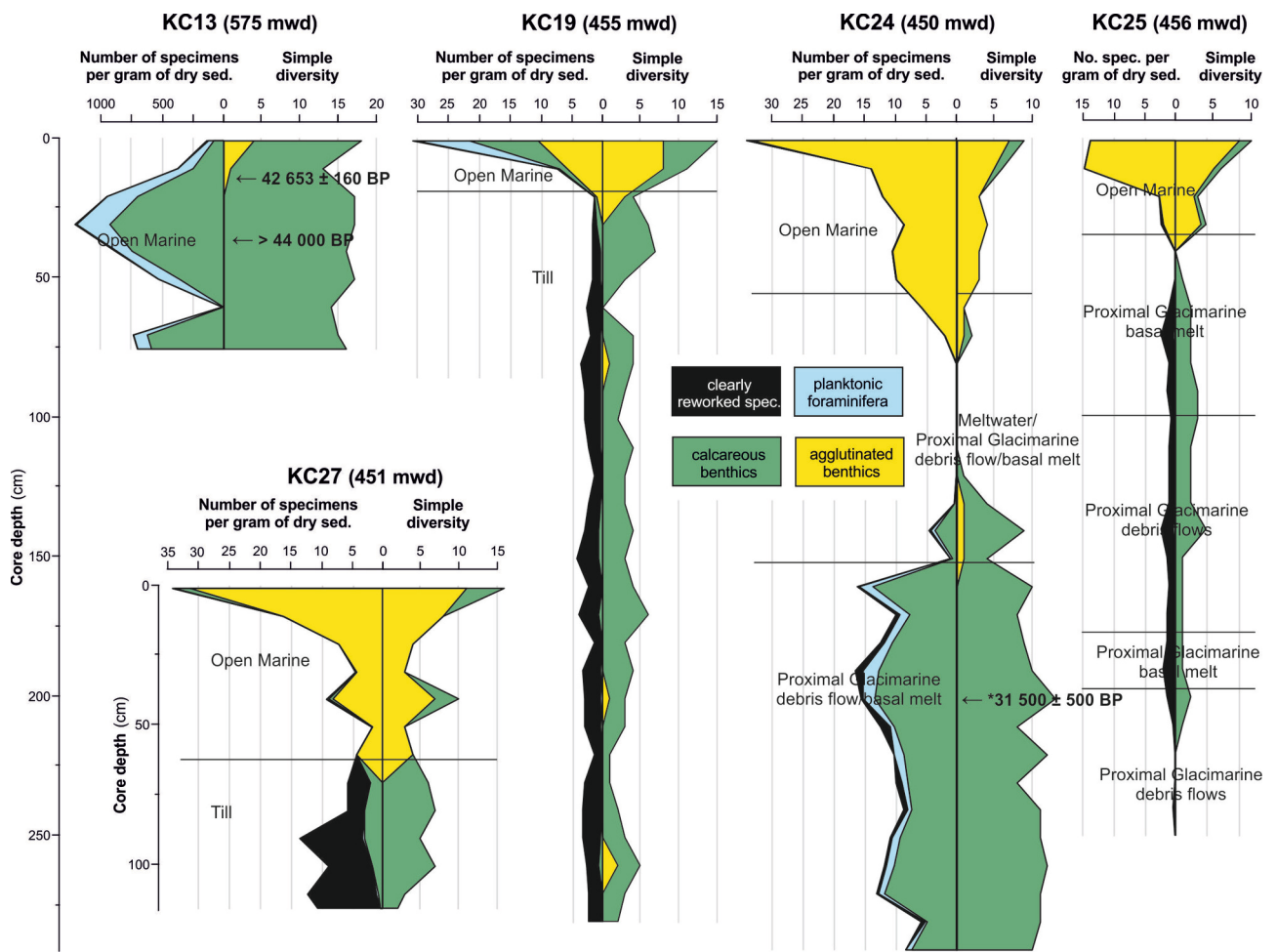
2019PA003716-f02-z-.jpg



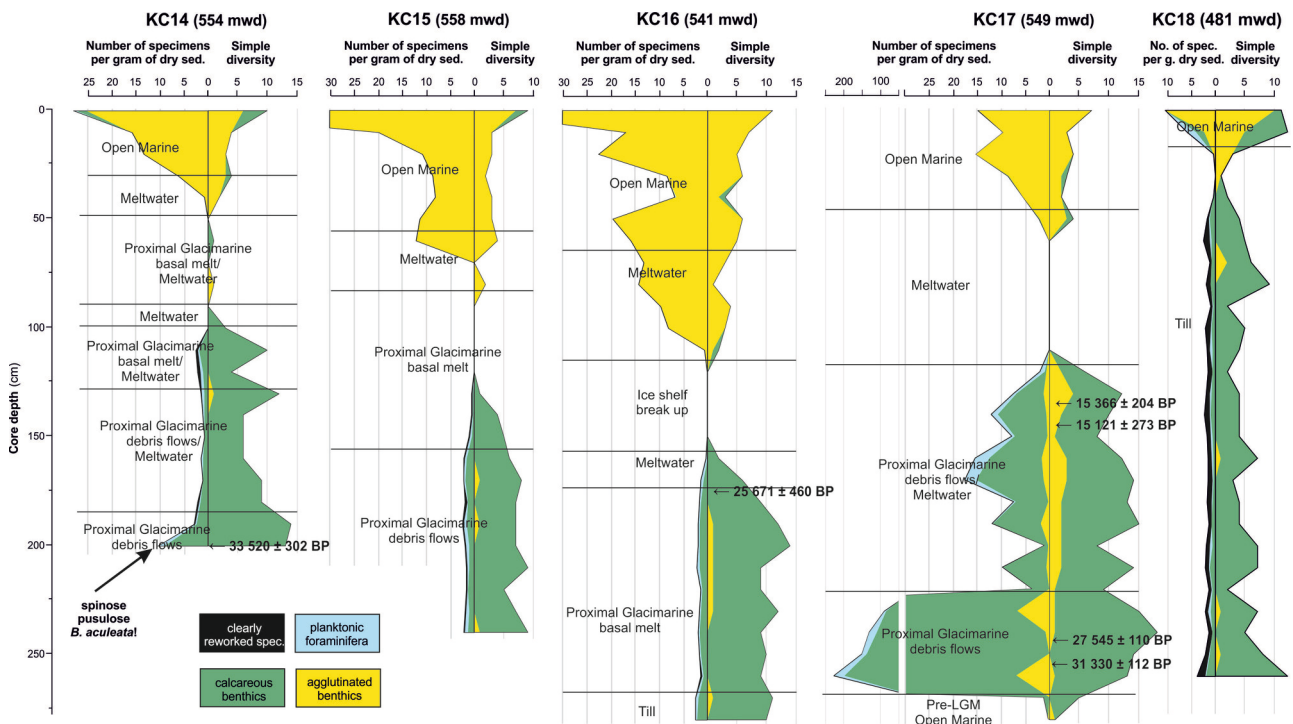
2019PA003716-f03-z-.jpg



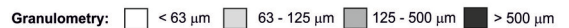
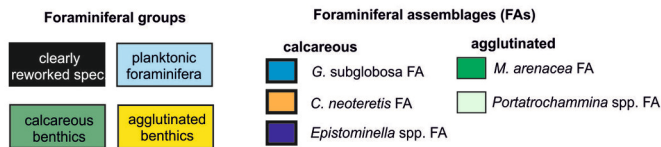
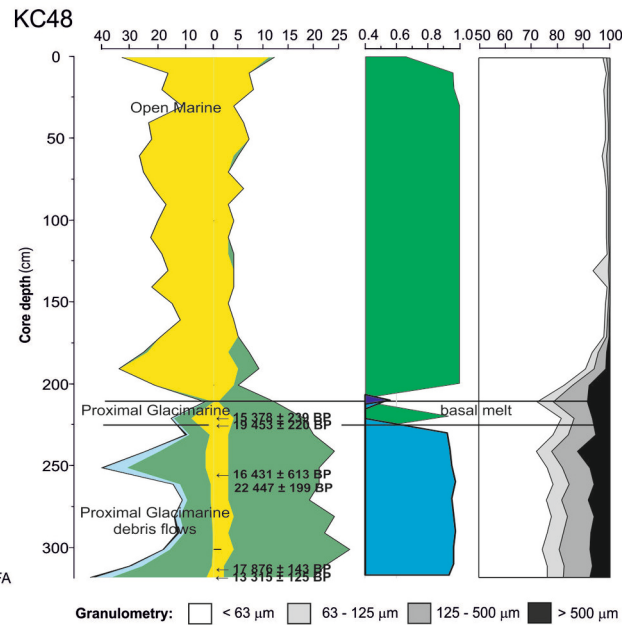
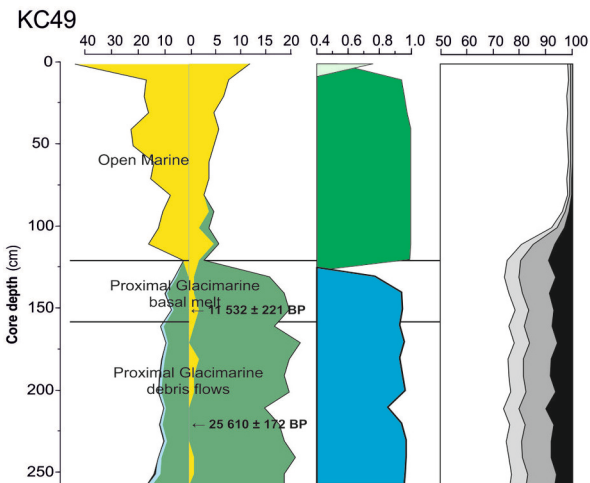
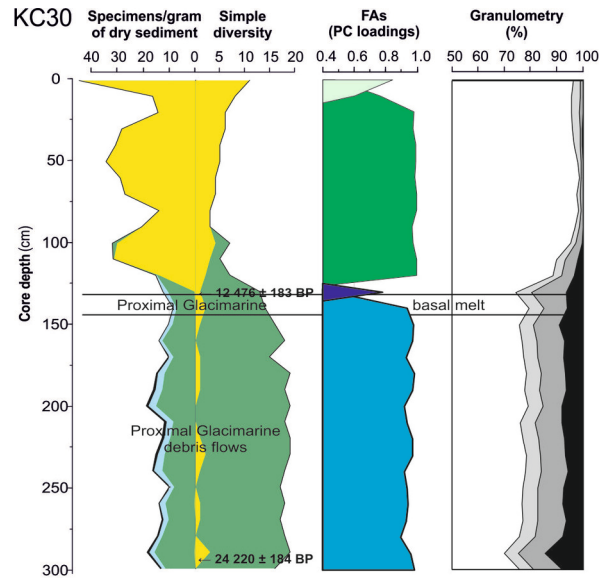
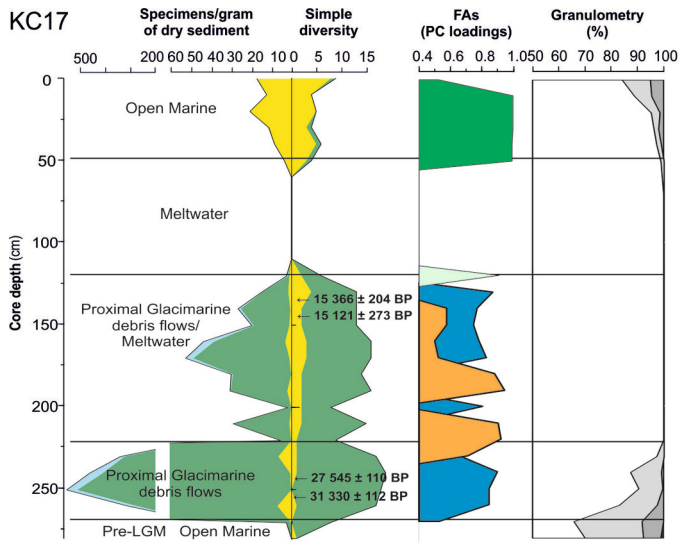
2019PA003716-f04-z.jpg



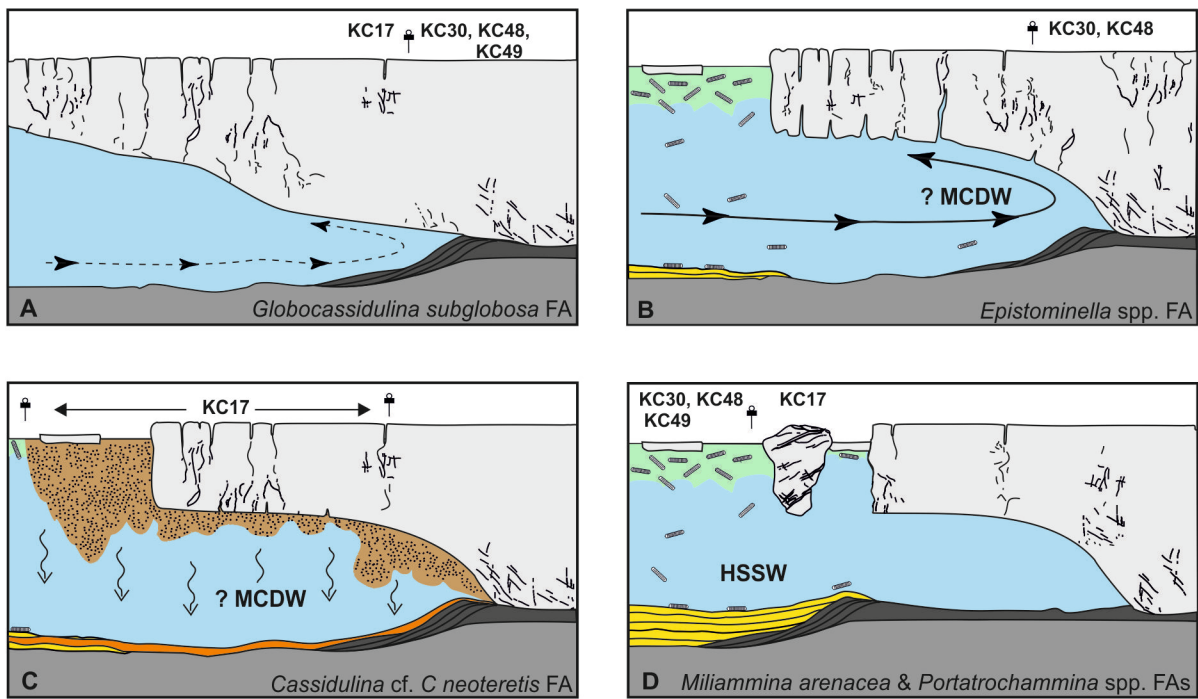
2019PA003716-f05-z-.jpg



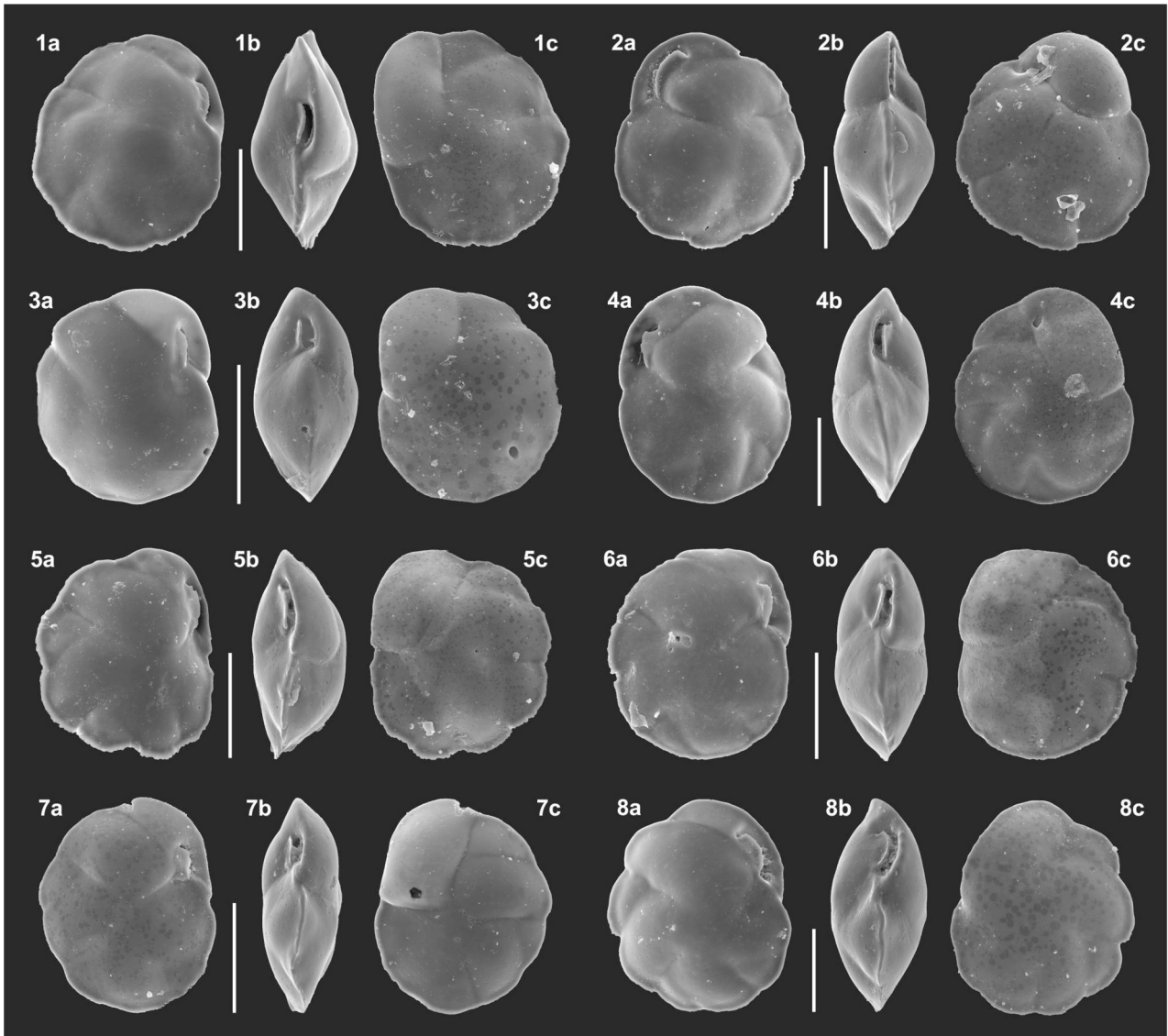
2019PA003716-f06-z-.jpg



2019PA003716-f07-z.jpg



2019PA003716-f08-z-.jpg



2019PA003716-f09-z-.jpg